PHYSIOLOGICAL PHARMACOKINETICS OF BIOLOGICALLY ACTIVE PEPTIDES: ROLES OF RECEPTOR BINDING AND ENDOCYTOSIS ON THE PHARMACOKINETICS OF OPIOID PEPTIDES AND INSULIN

BY

HITOSHI SATO

PHYSIOLOGICAL PHARMACOKINETICS OF BIOLOGICALLY ACTIVE PEPTIDES: ROLES OF RECEPTOR BINDING AND ENDOCYTOSIS ON THE PHARMACOKINETICS OF OPIOID PEPTIDES AND INSULIN

BY

HITOSHI SATO

FACULTY OF PHARMACEUTICAL SCIENCES,

KANAZAWA UNIVERSITY,

KANAZAWA, 1991

ACKNOWLEDGEMENTS

I would like to express my sincere appreciation to Professor Akira Tsuji for his fruitful guidance and endless encouragement he gave me consistently throughout my study. I would like to greatly thank Professor Manabu Hanano for his heartful education since the beginning of my graduate training. I am grateful to Dr. Tetsuya Terasaki for his earnest and abundant advice. I would like to express my gratitude to Dr. Tatsuji Iga for his warm education and accurate advice. I would like to express my appreciation to Dr. Yuichi Sugiyama for his excellent instruction that led me to pharmacokinetic research. I wish to thank Drs. Yasufumi Sawada, Hideyoshi Harashima and Ikumi Tamai for their warmest advice throughout my study. I would like to thank all the members of the Department of Pharmaceutical Sciences, Kanazawa University, for supporting me to accomplish my research. Finally, I would like to dedicate this thesis to my parents for their heartful endurance and affection they showed me during my research career.

TABLE OF CONTENTS

GENERAL INTRODUCTION

Recent progress in gene technology has enabled us to consider various bioactive polypeptides as candidates for therapeutic pharmaceuticals. Therefore, it is a matter of great importance to clarify the mechanisms underlying the elimination and distribution of these polypeptides, to evaluate their *vivo* efficacy in a quantitatively manner. Pharmacokinetic studies of biologically active peptides and proteins have been performed exclusively by compartment model analysis and moment analysis. Despite its potential clinical utility, however, either a compartmental model or a moment analysis cannot predict the time course of drug concentration in any target tissue, since it lacks anatomical and physiological reality in nature. On the other hand, by incorporating certain known or hypothetical mechanisms underlying the cellular distribution, uptake, and metabolism of a given drug in a physiological context, a physiological model can comprehensively predict drug concentrations in any anatomical regions of interest, including practically inaccessible biological fluids and specific sites of tissues. Thus, its utility has been demonstrated in quantitatively describing the elimination and distribution of various kinds of drugs.

Therefore, this thesis was undertaken to clarify the predominant factors that determine the elimination and distribution of biologically active peptides. For this purpose, I used ^{125}I-labeled opioid peptides and insulin as model polypeptides. First, I examined the effect of a transcapillary diffusional barrier for their tissue distribution. Second, I examined the effect of specific binding on their clearance and distribution, using *in vivo* system, isolated

perfused organ system, and *in vitro* isolated membrane system. Third, I examined the effect of receptor-mediated endocytosis and receptor recycling on hepatic insulin clearance and distribution. Finally, I developed a physiological pharmacokinetic model of insulin, considering 1) transcapillary diffusion, 2) receptor binding, 3) receptor-mediated endocytosis, 4) intracellular degradation, and 5) receptor recycling. Moreover, in this thesis, I applied high-performance chromatography (HPLC) to the determination of labeled insulin in biological samples. In order to overcome the analytical difficulty in discriminating an intact peptide and its degradation products, I propose that HPLC is a useful tool which has a greater resolving power than other methods.

PART I

PHYSIOLOGICALLY BASED PHARMACOKINETICS OF RADIOIODINATED HUMAN β-ENDORPHIN IN RATS: AN APPLICATION OF THE CAPILLARY MEMBRANE-LIMITED MODEL

SUMMARY

In order to simulate the distribution and elimination of radioiodinated human β-endorphin (^{125}I-β-EP) after iv bolus injection in rats, we proposed a physiologically based pharmacokinetic model incorporating diffusional transport of ^{125}I-β-EP across the capillary membrane. This model assumes that the distribution of ^{125}I-β-EP is restricted only within the blood and the tissue interstitial fluid, and that a diffusional barrier across the capillary membrane exists in each tissue except the liver. The tissue-to-blood partition coefficients were estimated from the ratios of the concentration in tissues to that in arterial plasma at the terminal (pseudoequilibrium) phase. The total body plasma clearance (9.0 ml/min/kg) was appropriately assigned to the liver and kidney. The transcapillary diffusion clearances of ^{125}I-β-EP were also estimated and shown to correlate linearly with that of insulin in several tissues. Numerically solving the mass-balance differential equations as to plasma and each tissue simultaneously, simulated concentration curves of ^{125}I-β-EP corresponded well with the observed data. It was suggested by the simulation that the initial rapid disappearance of ^{125}I-β-EP from plasma iv injection could be attributed in part to the transcapillary diffusion of the peptide.

INTRODUCTION

β-Endorphin (β-EP) (1), a straight chain polypeptide containing 31 amino acid residues, is an endogenous peptide that exhibits potent analgesic activity when administered intravenously (2) and intracerebroventricularly (3). Its function in the central nervous system has been linked with the analgesic activity (4). Since β-EP has been recently shown to depress cardiovascular (5) and respiratory (6) function and gastrointestinal motility (7), increasing attention has been paid to the direct endorphin action on peripheral tissues such as heart, lung, and small intestine, as well as to the central pharmacological actions.

Pharmacokinetic studies on peptide hormones including human β-endorphin (8-10) have been performed exclusively by noncompartmental or two- (three-) compartmental analyses. Even though these models are easy to handle and possess clinical practicability, these models cannot theoretically predict the concentration profiles of a drug in plasma or in a certain tissue when the physiological situations are altered in disease states, drug interaction, pregnancy, or aging. Recently, the utility of physiologically based pharmacokinetic models has been demonstrated in describing quantitatively the elimination and distribution of various drugs (11-16). These models are discriminated from the conventional compartmental models, because all compartments, interconnected with the blood flow, represent real organs or anatomic tissue regions in the body, and all parameters involved have a physiologically or physiochemically meaningful basis. In the present study, plasma disappearance and tissue distribution of radioiodinated human β-endorphin (^{125}I-β-EP) after iv bolus injection were examined by gel filtration and trichloroacetic acid precipitation methods, and

simulated using a physiologically based pharmacokinetic model incorporating a transcapillary diffusion in each tissue except the liver, namely the "capillary membrane-limited" physiological model. Even though the transcapillary diffusion of polypeptide hormones may be important for the mediation of hormonal actions in many tissues (17, 18), there is little information concerning the capillary membrane permeability of peptide hormones, except that across the blood-brain barrier (19, 20). Therefore, in the present study, we described a feasible method of estimating the transcapillary diffusion clearances and the interstitial fluid-to-blood partition coefficients of ^{125}I-β-EP for the various tissues from in vivo data and physiological constants so that we could simulate the concentration profiles of the peptide in the plasma and tissues examined. To our knowledge to data, this is the first demonstration of a physiologically based pharmacokinetic modeling of a peptide hormone.

MATERIALS and METHODS

Reagents. Human β-endorphin (β-EP) and trichloroacetic acid (TCA) were purchased from Wako Pure Chemical Industries, Ltd. (Osaka, Japan), Sephadex G-50 from Pharmacia Fine Chemicals (Uppsala, Sweden), and bovine serum albumin (fraction V) from Sigma Chemical Co. (St. Louis, MO). Trasylol was obtained from Bayer (Leverkusen, West Germany) and sodium iodide-125 (100 mCi/ml) from the Radiochemical Center (Amersham, Arlington Heights, IL). All other reagents were commercially available and of analytical grade.

Radioiodination. Immunoreactive radioiodinated human β-endorphin (^{125}I-β-EP), with a specific activity of 83 μCi/μg, was prepared as previously described (21). The labeled hormone was at least 95% pure as assayed by chromatography on Sephadex G-50 and stored at -20°C until study.

Drug Administration and Sampling. Adult male Wistar rats (Nihon Seibutsu Zairyo, Tokyo, Japan) weighing 240-320 g were used throughout the experiments. Food and water were available ad libitum. The bile duct and the bladder were cannulated with polyethylene tubing and, after recovery from ether anesthesia, approximately 8 μCi/kg of ^{125}I-β-EP plus saline up to 200 μl was rapidly injected through the femoral vein. Blood samples were withdrawn from the femoral artery at designated times (2, 5, 15, 30, and 60 min) after iv administration and were collected in heparinized tubes. Plasma was quickly separated from blood by centrifugation and stood on ice to avoid possible degradation of ^{125}I-β-EP in plasma. Bile and urine were sampled at time intervals. For tissue sampling, the rats were killed by cutting the carotid artery at designated times (2, 15, 30, and 60 min), and liver, kidney, lung, muscle, adipose, gut, heart, brain, and skin were

quickly excised, rinsed with ice-cold saline, blotted dry, and a portion of each tissue was weighed and counted for the total radioactivity in a gamma-counter (model ARC-300, Aloka Co., Ltd., Tokyo, Japan) with a counting efficiency of approximately 80%. Another portion (about 0.5 g) was quickly added to 5 ml of ice-cold 20% v/v acetic acid solution containing 0.01 M ammonium acetate (designated as AcOH solution) and stored at -40°C until assay.

TCA Precipitation Method. Plasma, urine, or bile samples (50-200 µl) were added to 2 ml of ice-cold 15% w/v trichloroacetic acid containing 0.1% w/v bovine serum albumin (designated as TCA solution) and mixed well. After standing at 4°C for 30 min, the mixture was centrifuged at 3000 rpm for 30 min, and the supernatant was transferred to a separate tube by aspiration. The percentage of radioactivity in precipitate (designated as TCA-precipitable %) was calculated as (cpm in precipitate) / {(cpm in precipitate) + (cpm in supernatant)} x 100. Some of these samples were chromatographed on a Sephadex G-50 column (1 X 45 cm) eluted with AcOH solution, and the percentage of radioactivity associated with intact ^{125}I-β-EP was calculated by measuring the peak areas eluted from the column. To determine tissue concentrations of intact ^{125}I-β-EP, each tissue was homogenized in AcOH solution in a motor-driven Potter homogenizer, and 1 ml of the homogenate was added to 1 ml of 30% w/v trichloroacetic acid. The subsequent procedure was the same as described above for plasma, urine, and bile samples. TCA-precipitable % and chromatographically intact % of ^{125}I-β-EP in these biological samples were correlated to validate the TCA precipitation method.

Blood-to-Plasma Partition Coefficient (R_B). Blood was sampled via

the carotid artery into a heparinized tube and pooled from five rats. An aliquot (0.5 ml) of the blood was transferred to an open flask, supplied O_2 gas, and preincubated for 5 min at 37°C prior to the addition of ^{125}I-β-EP (about 50,000 cpm/ml). To examine the equilibration time between the plasma and blood cells, 100 µl of the blood was quickly separated by centrifugation 6, 11, 15, and 30 min after the addition of ^{125}I-β-EP. The radioactivity of intact ^{125}I-β-EP in plasma and in blood cells was determined by the TCA precipitation method, respectively. To examine the concentration dependency of R_B, another portion (0.5 ml) of blood was also incubated with ^{125}I-β-EP in the presence of 0, 1, 10, and 100 nM unlabeled β-EP at 37°C for 15 min. Subsequent procedure was determined by centrifugation at 3,000 rpm for 15 min in a closed glass capillary. R_B was calculated by R_B = {1 + (intact cpm in blood cells)/(intact cpm in plasma)} x (1 - Ht).

Data Calculations. Concentrations of ^{125}I-β-EP in biological samples were expressed as percentage of dose per ml of samples, i.e. (intact cpm/ml of sample)/(intact cpm injected/kg of body weight). Tissue-to-arterial plasma concentration ratios were calculated as (intact cpm/ml of tissue)/(intact cpm/ml of plasma) and converted to tissues-to-arterial blood concentration ratios (Kp_{app}) by dividing by R_B.

Model Development. A physiologically based pharmacokinetic model for the distribution, metabolism and excretion of ^{125}I-β-EP in rats was depicted in fig. 1. The model consists of nine tissues and blood compartments, which represent real organs or anatomic tissue regions in the body. It is assumed that ^{125}I-β-EP is metabolized and excreted by liver and kidney, respectively. Fig. 2 is the schematic

representation of a one- organ model of an eliminating organ subdivided anatomically into the three fluid compartments, i.e. the capillary bed, the interstitial fluid (designated as ISF), and the intracellular space. This model assumed that: 1) each compartment constituting a whole organ is well stirred, 2) binding equilibrium of ^{125}I-β-EP in the capillary bed and ISF is instantaneously established, 3) the distribution of ^{125}I-β-EP is restricted only within extracellular fluids, i.e., blood and ISF, 4) the distribution of ^{125}I-β-EP is limited by the diffusion process across the capillary membrane in each tissue except the liver, and 5) only the unbound ^{125}I-β-EP is subject to the transcapillary diffusion, metabolism, and excretion. In the liver , the distribution of ^{125}I-β-EP is assumed to be blood-flow limited, i.e., a rapid equilibrium between the capillary bed and ISF occurs. The unbound concentration of ^{125}I-β-EP in the capillary bed and in ISF for i-type tissue is expressed as follows, respectively:

$$C_{Bi,u} = f_B C_{Bi} \quad (1)$$

$$C_{ISi,u} = f_{ISi} C_{ISi} \quad (2)$$

where C_{Bi}, $C_{Bi,u}$, and f_B are the total concentration, unbound concentration, and unbound fraction of ^{125}I-β-EP in the capillary bed, respectively; C_{ISi}, $C_{ISi,u}$, and f_{ISi} are the total concentration, unbound concentration, and unbound fraction of ^{125}I-β-EP in ISF, respectively.

The interstitial fluid-to-blood partition coefficient (Kp_i^*) is defined as:

$$Kp_i^* = C_{ISi,ss}/C_{Bi,ss} \quad (3)$$

where $C_{ISi,ss}$ and $C_{Bi,ss}$ are the steady state concentrations in the

capillary bed and in ISF, respectively. At steady state, the unbound concentrations in both fluid compartments are equivalent, because a simple diffusion (not an active transport) across the capillary membrane is assumed. Therefore Kp_i^* is also expressed as:

$$Kp_i^* = f_B/f_{ISi} \quad (4)$$

Based on the concept of mass balance, the differential equations describing the concentrations of ^{125}I-β-EP in *i*-type tissue (an eliminating organ) are given as follows (see Appendix II for a complete set of equations):

$$V_{Bi}(dC_{Bi}/dt) = Q_i(C_a - C_{Bi}) - P_i f_B(C_{Bi} - C_{ISi}/Kp_i^*) \quad (5)$$

$$V_{ISi}(dC_{ISi}/dt) = P_i f_B(C_{Bi} - C_{ISi}/Kp_i^*) - f_B CL_{inti} C_{ISi}//Kp_i^* \quad (6)$$

where Q_i is the blood flow rate, C_a is the concentration of ^{125}I-β-EP in arterial blood, V_{Bi} and V_{ISi} are the volumes of the capillary bed and ISF, respectively, P_i and CL_{inti} are the transcapillary diffusion clearance and intrinsic metabolic clearance, respectively. For a noneliminating organ, CL_{inti} is set equal to 0. C_{ISi}, Kp_i^*, and V_{ISi} are expressed as:

$$C_{ISi} = C_{Ti}/VR_i \quad (7)$$

$$Kp_i^* = Kp_i/VR_i \quad (8)$$

$$V_{ISi} = VR_i V_{Ti} \quad (9)$$

where C_{Ti} is the tissue concentration of ^{125}I-β-EP which is directly measured in the experiment, VR_i is the volume ratio the interstitial fluid (V_{ISi}) to the whole tissue (V_{Ti}) excluding the capillary bed, Kp_i is the tissue-to-blood partition coefficient of ^{125}I-β-EP. Substituting C_{ISi} and Kp_i^* in equations 5 and 6 according to equations 7-9 gives:

$$V_{Bi}(dC_{Bi}/dt) = Q_i(C_a - C_{Bi}) - P_i f_B(C_{Bi} - C_{Ti}/Kp_i) \quad (10)$$

$$V_{Ti}(dC_{Ti}/dt) = P_i f_B(C_{Bi} - C_{Ti}/Kp_i) - f_B CL_{inti} C_{Ti}/Kp_i \quad (11)$$

As concerns the renal handling of the peptide, ^{125}I-β-EP is supposed to be filtered at the glomeruli into the renal tubules, followed by enzymatic degradation in the proximal tubules. Therefore, the mass balance equations describing the concentrations or amount of ^{125}I-β-EP in the capillary bed, ISF, renal tubules, and whole kidney tissue are given as follows, respectively:

$$V_{B,R}(dC_{B,R}/dt) = Q_R(C_a - C_{B,R}) - f_B GFR \cdot C_a - P_R f_B(C_{B,R} - C_{IS,R}/Kp_R^*) \quad (12)$$

$$V_{IS,R}(dC_{IS,R}/dt) = P_R f_B(C_{B,R} - C_{IS,R}/Kp_R^*) \quad (13)$$

$$dX_{RT}/dt = f_B GFR \cdot C_a - kdX_{RT} - dX_u/dt \quad (14)$$

$$V_{T,R}C_{T,R} = V_{IS,R}C_{IS,R} + X_{RT} \quad (15)$$

where GFR is the glomerular filtration rate (or inulin clearance), X_{RT} is the amount of ^{125}I-β-EP in the renal tubules, X_u is the cumulative amount excreted in urine, kd is the degradation rate constant in the renal tubules by hydrolytic enzymes, and $C_{T,R}$ is the average concentration in the kidney.

For each tissue except the liver, Kp of ^{125}I-β-EP is expressed as a function of P and K_{app} by the equations in Appendix I (an extension of the method proposed by Chen and Gross (22) in which the general equations were derived to estimate the values of P and Kp for all tissues at the pseudoequilibrium condition. When the values of P and Kp at the steady state condition are needed, the term z should be set at 0 in each equation. The value of P was estimated by curve-fitting using a hybrid model (23), and the value of Kp was simultaneously determined by equation A17 for the kidney, equation A22 for the liver, equation A26 for the lung, and A9 for the other tissues examined, respectively. Briefly, arterial blood concentration vs. time curve

was fitted to a biexponential equation by a nonlinear least squares regression (24). Therefore, the input function to an organ was represented without the necessity of modeling the whole body system. The equation described the concentration in an organ was analytically solved by a Laplace transformation and the unknown parameters (P and Kp) concerning the organ were estimated by fitting the solved equation to the observed data. Only for the kidney, the value of kd as well as P and Kp was simultaneously estimated by curve-fitting.

RESULTS

Gel Filtration and TCA Precipitation of ^{125}I-β-EP in Biological Samples. Fig. 3 shows the chromatographic separation of ^{125}I-β-EP on Sephadex G-50 from rat plasma after iv bolus injection of tracer dose (approximately 8 μCi/kg) with (below) and without (above) 168 μg/kg of unlabeled β-EP. Three radioactive peaks eluted from the column. The first, eluting at the void volume, is supposed to consist of ^{125}I-β-EP degradation products with a molecular weight higher than that of ^{125}I-β-EP itself. The second peak was associated with intact ^{125}I-β-EP. The third peak corresponded to low molecular weight degradation products. The percentage of the radioactivity associated with intact ^{125}I-β-EP decreased with time, indicating that metabolism of ^{125}I-β-EP was proceeding. There was no difference in the extent of metabolism of ^{125}I-β-EP in the presence and absence of unlabeled β-EP, since the percentage of radioactivity eluting at the third peak is not different with each other. Fig. 4 shows the chromatographic separation of ^{125}I-β-EP on Sephadex G-50 from urine (top) and bile (bottom) after the injection of tracer doses (approximately 8 μCi/kg). Approximately 30% of the radioactivity remained intact in the urine collected 0-10 min after the injection, while no intact radioactivity was excreted into urine thereafter. Intact ^{125}I-β-EP was not excreted into bile throughout the sampling interval. The total radioactivity recovered in urine and bile for 3 hr was approximately only 3% of the injected dose, respectively. Therefore, we neglected the last term of equation 14, dX_U/dt, and accordingly derived the equations to estimate the Kp value of ^{125}I-β-EP for the kidney in Appendix I.

A good correlation was observed between TCA-precipitable % and chromatographically intact % of ^{125}I-β-EP in plasma, urine, and bile

samples and tissue homogenate (N = 15). The obtained regression line was $y = 0.922x + 7.68$ ($r = 0.988$, $p < 0.001$). Since the chromatographic method is more reliable and authorized than the TCA precipitation method, the TCA-precipitable % of ^{125}I-β-EP was corrected to chromatographically intact % by this regression line and used in the present pharmacokinetic study.

Blood-to-Plasma Partition Coefficient (R_B). Fig. 5A shows that the distribution of ^{125}I-β-EP in blood cells reached steady state within 5 min after the addition of the labeled peptide. R_B of ^{125}I-β-EP was determined to be 0.73 ± 0.02 (mean ± SD; N=4) at 37°C. As shown in fig. 5B, the distribution of ^{125}I-β-EP to the blood cells was concentration-independent over the concentration range studied (1-100 nM). We previously reported that the unbound fraction of ^{125}I-β-EP in serum (f_p) was 0.6 and constant over the same concentration range. Consequently, the unbound fraction of ^{125}I-β-EP in blood (f_B) was calculated as $f_p/R_B = 0.82$.

Physiologically Based Pharmacokinetic Modeling. In the present pharmacokinetic study, near complete recovery of the administered dose of radioactivity (more than 85%) from blood, tissues, bile, and urine was achieved at each sampling time. As shown in table 1, the pharmacokinetic parameters or constants of ^{125}I-β-EP were not significantly different between the rats injected with and without 168 μg/kg of unlabeled β-EP. Therefore, the parameters obtained without unlabeled β-EP were used in the analysis thereafter. The total body clearance of ^{125}I-β-EP was 12.3 ± 4.2 ml/min/kg (mean ± SE; N =3). On the other hand, ^{125}I-β-EP was degraded in plasma and blood at 37°C in vitro with the half-lives ($t_{1/2}$) of 7.5 and 4.0 hr, respectively.

Expressed as the unit of clearance, these in vitro degradation rates correspond to 0.065 and 0.23 ml/min/kg, calculated as V x $\ln 2/t_{1/2}$ (V is the plasma and blood volume in the body), respectively.. Therefore, we neglected the contribution of these clearance to the total body blood clearance . By our liver perfusion experiment using single-pass isolated rat liver preparations, the hepatic extraction ratio (E_H) of ^{125}I-β-EP at steady state was determined to be 0.29 (the mean of two preparations). Therefore, the hepatic blood clearance (CL_H) of ^{125}I-β-EP was calculated as $Q_H \times E_H$ = 8.2 ml/min/kg, where Q_H is the hepatic blood flow rate. When ^{125}I-β-EP is assumed to be metabolized or eliminated predominantly by liver and kidney, the extrahepatic clearance (4.1 ml/min/kg) is assigned to the kidney. Thus, assigned renal blood clearance (CL_R) is equal to the product of the glomerular filtration rate (GFR; 5 ml/min/kg)(15) and f_B of ^{125}I-β-EP (0.82). This coincidence suggests that the major eliminating organs of ^{125}I-β-EP in rats may be liver and kidney. The hepatic blood clearance was converted to the hepatic intrinsic clearance ($CL_{int,H}$) by the following equation, assuming that the liver conforms to a "well-stirred" model (25).

$$CL_{int,H} = Q_H CL_H / f_B / (Q_H - CL_H) \quad (16)$$

The initial distribution volume (V_1) was 59.2 ± 2.5 ml/kg (mean ± SE; N = 3), which is close to the the plasma volume in rats. The steady state distribution volume (Vd_{SS}) was 168 ± 12 ml/kg (mean ± SE; N = 3), which is close to the sum of the tissue extracellular spaces (see table 2). Fig.6 shows the relationship between the transcapillary diffusion clearances (P) of ^{125}I-β-EP and those of inulin for the muscle, gut, skin, lung, and heart (15), expressed as the diffusion clearance per whole tissue. A linear relationship was found between

the P values of ^{125}I-β-EP and inulin in the several tissues. The regression line was $y = 1.07x - 0.26$ ($r = 0.986$, $p < 0.005$). As shown in fig. 7, A-D, concentrations of ^{125}I-β-EP in plasma and tissues 60 min after iv injection were almost in the terminal phase and therefore the derived equations in Appendix I could be properly applied to estimate the Kp values. As shown in table 2, the estimated values of Kp were as small as inulin spaces for the heart, muscle, skin, and adipose, 2- or 3-fold for the lung, liver, kidney, and gut, and several fold for the brain. The estimated values of P were one-third of the tissue blood flow for the kidney, muscle, and gut, and less than one-tenth for the other tissues examined. For the kidney, the rate of degradation of ^{125}I-β-EP at the renal tubules was estimated to be 0.3 (% dose/min) by curve-fitting using a hybrid model. Thus obtained values of Kp and P of ^{125}I-β-EP for each tissue were listed in table 1 together with physiological constants for a male Wistar rat (240 g), i.e. the tissue volume, capillary bed volume (as the blood volume), interstitial space (% of the tissue volume), and blood flow rate. These physiological parameters and constants were used in the present simulation by a physiologically based pharmacokinetic model. The simultaneous differential equations (in Appendix II) for all compartments were solved numerically by the Runge-Kutta-Gill method using a digital computer at a suitable interval (0.005 min). The obtained simulation curves for plasma and various tissues were presented in fig. 7, A-D. Note that the ordinate indicates the plasma concentration of the peptide (cpm/ml) divided by the dose (cpm/kg), so that it means that a 240-g rat was injected with 24 % of the dose. To examine the recovery of the pharmacokinetic constants by the

simulation, we fitted the five points of the simulated plasma concentrations (2,5,15,30, and 60 min after iv injection) to a biexponential equation by a nonlinear least squares regression (24), and the recovered pharmacokinetic parameters were calculated using the conventional equations (27) and included in table 2.

DISCUSSION

The present study was designed to quantitate the pharmacokinetic behavior of β-EP in rats based on the physiological parameters and constants, although it has a methodological limitation that gel filtration does not have the resolving power to differentiate between the intact peptide and its metabolites shortened by one or two amino acids, in constant to reversed-phase HPLC (28).

Urinary and biliary excretion of ^{125}I-β-EP was negligible, because only 3% radioactivity of the injected dose was recovered in urine and in bile, respectively. Moreover, intact ^{125}I-β-EP was excreted only in the urine collected 0-10 min after iv injection. These results suggest that ^{125}I-β-EP ultrafiltered at kidney glomeruli may be reabsorbed in the proximal tubules and thereafter exposed to lysosomal degradation, as supposed to be the general mechanism concerning renal handling of polypeptide hormones (29). The partition of ^{125}I-β-EP to blood cells at 37°C was shown to be time-independent, while the intact percentage of ^{125}I-β-EP in plasma and blood slowly decreased with the half-lives of 7.5 and 4.0 hr, respectively. Moreover, the value of R_B was concentration-independent over the range studied (1-100 nM), indicating that there was no specific binding of ^{125}I-β-EP on the blood cells.

The tissue distribution of ^{125}I-β-EP was assumed to be limited only to the blood and ISF, because the Kp values were as small as inulin spaces for all tissues. In such a case, arbitrary contamination of blood into sampled tissues is a serious problem. Therefore, in the present study, we shed as much blood as possible from the carotid artery before we removed tissues and carefully rinsed the sampled tissues in cold saline and blotted them dry. Little contamination of

red blood cells was observed when the tissues were homogenized prior to the TCA precipitation. On the other hand, if an animal is killed by a rapid injection of air into the intravenous cannula, blood will necessarily remain in the tissues, so that we must take the remaining blood into consideration in a pharmacokinetic analysis.

Polypeptide hormones, as well as other macromolecules and highly ionized compounds, are generally assumed to be impermeable through the tissue membrane, except in some transport systems such as endocytosis. First, we developed a physiologically based pharmacokinetic model assuming a rapid equilibrium between the blood and ISF,i.e. a blood flow-limited distribution into tissues. However, the model failed to provide an adequate simulation of the observed data. Obtained simulations considerably overestimated the tissue concentrations at early times, because the flow-limited model predicted that distribution equilibrium should be achieved at least within a few minutes after iv bolus injection. As previously discussed by Mintun et al. (12), a slow distribution (on a time scale of hours) of drugs can occur only when $Q_T/(KpV_T) < \lambda_z$, where Q_T is the tissue blood flow, V_T is the tissue volume, and λ_z is the slope of the terminal exponential phase of the plasma disappearance curve. However, such a condition does not hold in the case of ^{125}I-β-EP, because the Kp values of ^{125}I-β-EP were as small as the inulin spaces in all tissues. Therefore, we adopted a new model which includes a diffusion process between the capillary bed and ISF, namely the capillary membrane-limited model. Effects of a diffusional barrier across hepatocytes on drug metabolism have been described by us and others (30-32). In the present study, a diffusional barrier across the capillary membrane was

incorporated into a physiologically based pharmacokinetic model of ^{125}I-β-EP, because a rapid equilibrium between the capillary bed and ISF in most tissues except the liver cannot be assumed for relatively high molecular weight substances, e.g. inulin (33,34), dextrans, and albumin (35,36). As for the liver, it is expected that free exchange of materials between the capillary bed and extracellular fluid (in the space of Disse) would occur through its open fenestrae (37), while obvious filtration effects can be expected when particles of about the size of the fenestrae (approximately 0.1 μm) arrive in the liver (38).

McNamara et al. (39) described the effect of protein binding of drugs in ISF on the steady state distribution volume. In the present study, the ratio of the unbound fraction in blood (f_B) to that in ISF (f_{IS}) was expressed as the interstitial fluid-to-blood partition coefficient (Kp^*). Here, the binding of ^{125}I-β-EP in ISF means the binding to plasma proteins, red blood cells, and tissue cell membranes. As listed in table 2, the Kp value of ^{125}I-β-EP for the brain was estimated to be 0.024 and was close to that of β-[D-Ala^2,^{14}C-homoarginine]μ-endorphin reported by Rapoport et al. (19). On the other hand, the P value of ^{125}I-β-EP for the brain (1.2 g) was estimated to be 0.0035 ml/min and was not close to the permeability (0.0576 ml/min) calculated from their data, but comparable to the simple diffusion clearance of β-EP (0.012 ml/min) reported by Sharma and Vimal (20). As shown in fig. 6, the P values of ^{125}I-β-EP obtained in the present study are linearly correlated with those of inulin for several tissues. This correlation might happen because the molecular weight of ^{125}I-β-EP (3,600) is of the same order with that of inulin (5,000). Moreover, the P value of ^{125}I-β-EP for the kidney (2 g) was estimated to be 4.5 ml/min and approximately two-thirds of

that of inulin determined for rat kidneys by the multiple indicator dilution method (34). Since little is known about the transcapillary permeability of a peptide hormone in peripheral tissues except that of insulin in the dog hindlimb (one-half of the permeability coefficient of inulin) (17), our method of estimating the diffusion clearances from in vivo data together with the physiological and physicochemical constants will provide useful and valuable information concerning the pharmacokinetic behavior of peptide hormones.

As shown in fig. 7A, the simulated plasma concentration curve showed a good agreement with the observed values. Among the recovered pharmacokinetic constants (table 3), the recovered Vd_{ss} and CL_{tot} were in good agreement with the original values of Vd_{ss} and CL_{tot}, respectively, while the recovered V_1 is 45% larger than the original value. The resulting half-life of the initial phase was 2.1 min and corresponded well with the observed half-life, 2.3 min. When we added an earlier point of the simulated data for curve-fitting, such as at 1 min, the calculated value of V_1 was reduced to 58.5 ml/kg and almost equal to the original value, since the estimation of V_1 is sensitive to the earliest sampling point. Fig. 8 presents the observed plasma concentration 2, 5, and 15 min after iv injection and the predicted concentration curves simulated in the blood flow-limited and diffusion-limited models, respectively. The curve predicted by a flow-limited model underestimates the observed values, reflecting the rapid distribution of ^{125}I-β-EP into the tissue interstitial fluids from blood. Therefore, the blood flow-limited model failed to provide an adequate simulation of not only the concentration profiles of ^{125}I-β-EP in the tissues, but also the plasma disappearance curve. Let us

define the apparent influx clearance ($CL_{influxi,app}$) into i-type tissue as follows:

$$CL_{influxi,app} = Q_{Ti}f_B/(Q_{Ti} + f_BP_i) \quad (17)$$

Provided that the efflux rate is very small as compared with the blood flow, this parameter represents the initial uptake rate by the tissue, depending upon both f_BP_i and Q_{Ti}, and approximates to P_i in a membrane-limited case ($f_BP_i << Q_{Ti}$). The values of $CL_{influxi,app}$ of ^{125}I-β-EP for all tissues summed to 5.8 ml/min/240-g rat, which is 2-fold larger than the sum of organ clearances (2.9 ml/min/240-g rat). Taken all together, it was suggested by the present simulation study that the initial rapid decline of ^{125}I-β-EP in plasma after iv bolus injection would be, in part, attributed to the transcapillary diffusion of ^{125}I-β-EP into ISF. The same interpretation may be applied to the pharmacokinetic behavior of other polypeptide hormones such as insulin (40). It is interesting to note that, for many peptide hormones, half-lives of the initial rapid disappearance from plasma show 2-8 min (40) in various animal species. This suggests that the similar half-lives were caused, in part, by the transcapillary diffusion of the peptide into tissue interstitial fluids, depending upon the magnitude of transcapillary diffusion clearances.

As shown in fig.7B, ^{125}I-β-EP was accumulated in the kidney up to the concentration of more than 2-fold of that in plasma, which has been also observed for many peptide hormones (40). In the present simulation, we ascribed this accumulation in the kidney to both the binding of ^{125}I-β-EP in ISF ($f_{IS,R} = f_p/Kp_R^* = 0.25$) and the retention of filtered ^{125}I-β-EP in the renal tubules prior to the degradation by hydrolytic enzymes. However, we cannot exclude the possibility that

^{125}I-β-EP was reabsorbed at the renal tubules by endocytosis and thereafter exposed to lysosomal degradation, as is the case with insulin and lysozyme (29).

As presented in table 2, the pharmacokinetic parameters or constants of ^{125}I-β-EP determined from a two-compartment model were not altered in the presence of 168 μg/kg of unlabeled β-EP. This means a lack of dose dependency in the pharmacokinetics of ^{125}I-β-EP. However, the postdistributive half-life of β-EP obtained in the present study (32 min) is fairly different from that in our previous study (6.2 hr) in which β-EP was assayed by a radioreceptor assay (10), even though the same dose (168 μg/kg) of unlabeled β-EP was injected in either study. There might be two possible explanations for this discrepancy. The first explanation is that there is methodological difference derived by possible active metabolites of β-EP circulating in plasma, because radioreceptor assays recognize all the biological activity arising from both an intact drug and metabolites. This explanation is compatible with the observation that the initial half-lives of ^{125}I-β-EP were almost the same between the present (2.3 min) and previous (2.6 min) studies, since metabolism was not so prevailing during the distributive phase. The second explanation is that the pharmacokinetic behavior of immunoreactive ^{125}I-β-EP is different from that of unlabeled β-EP. In any case, further investigation is needed to clarify the reason for this discrepancy.

In conclusion, we developed a physiologically based pharmacokinetic model for radioiodinated human ^{125}I-β-EP in rats, in which the transcapillary diffusion clearances and the tissue-to-blood partition coefficients of the peptide were estimated from the concentration

profiles of ^{125}I-β-EP in plasma and tissues after iv bolus injection. Obtained simulation curves corresponded well with the observed data. It was suggested by the simulation that the rapid decline of the plasma concentration of ^{125}I-β-EP after iv injection could be attributed in part to the transcapillary diffusion into the tissue interstitial fluids, followed by the post distributive elimination phase.

REFERENCES

1. C. H. Li and D. Chung: Isolation and structure of an untriakontapeptide with opiate activity from camel pituitary glands. *Proc. Natl. Acad. Sci. U.S.A.* **73**, 1145-1148 (1976).
2. L. F. Tseng, H. H. Loh, and C. H. Li: β-Endorphin as a potent analgesic by intravenous injection. *Nature* **263**, 239-240 (1976).
3. H. H. Loh, L. F. Tseng, E. Wei, and C. H. Li: β-Endorphin is a potent analgesic agent. *Proc. Natl. Acad. Sci. U.S.A.* **73**, 2895-2898 (1976).
4. L. F. Tseng and J. M. Fujimoto: Differential actions of intrathecal naloxone on blocking the tail-flick inhibition induced by intraventricular β-endorphin and morphin in rats. *J. Pharmacol. Exp. Ther.* **232**, 74-79 (1985).
5. J. W. Holaday: Cardiovascular consequences of endogenous opiate antagonism. *Biochem. Pharmacol.* **32**, 573-585 (1983).
6. J. Florez, A. Mediavilla, and A. Pazos: Respiratory effects of β-endorphin, D-ala^2-met-enkephalinamide, and met-enkephalin injected into the lateral ventricle and the pontomedullary subarachnoid space. *Brain Res.* **199**, 197-206 (1980).
7. T. P. Davis, A. J. Culling, H. Schoemaker, and J. J. Galligan: β-Endorphin and its metabolites stimulate motility of the dog small intestine. *J. Pharmacol. Exp. Ther.* **277**. 499-507 (1983).
8. K. M. Foley, I. A. Kourides, C. E. Inturrisi, R. F. Kaiko, C. G. Zaroulis, J. B. Posner, R. W. Houde, and C. H. Li: β-Endorphin. Analgesic and hormonal effects in humans. *Proc. Natl. Acad. Sci. U.S.A.* **76**, 5377-5381 (1979).
9. N. Aronin, M. Wiesen, A. S. Liotta, G. C. Schussler, and D. T. Krieger: Comparative metabolic clearance rates of β-endorphin and β-lipotropin in humans. *Life Sci.* **29**, 1265-1269 (1981).

10. H. Sato, Y. Sugiyama, Y. Sawada, T. Iga, and M. Hanano: Pharmacokinetic study of exogenously administered β-endorphin using a rapid radioreceptor assay in rats. *Life Sci.* **35**, 1051-1059 (1984).
11. K. B. Bishoff and R. L. Dedrick: Thiopental pharmacokinetics. *J. Pharm. Sci.* **57**, 1346-1351 (1968).
12. M. Mintun, K. J. Himmelstein, R. L. Schroder, M. Gibaldi, and D. D. Shen: Tissue distribution kinetics of tetraethylammonium ion in the rats. *J. Pharmacokin. Biopharm.* **8**, 373-409 (1980).
13. J. M. Engasser, F. Sarhan, C. Falcoz, M. Minier, P. Letourneur, and G. Siest: Distribution, metabolism, and elimination of phenobarbital in rats. Physiologically based on pharmacokinetic model. *J. Pharm Sci.* **70**, 1233-1237 (1981).
14. J. H. Lin, Y. Sugiyama, S. Awazu, and M. Hanano: Physiological pharmacokinetics of ethoxybenzamide based on biochemical data obtained in vitro as well as on physiological data. *J. Pharmacokinet. Biopharm.* **10**, 649-661 (1982).
15. A. Tsuji, T. Yoshikawa, K. Nishide, H. Minami, M. Kimura, E. Nakashima, T. Terasaki, E. Miyamoto, C. H. Nightingale, and T. Yamana: Physiologically based pharmacokinetic model for β-lactam antobiotics. I. Tissue distribution and elimination in rats. *J. Pharm. Sci.* **72**, 1239-1251 (1983).
16. L. E. Gerlowski and R. K. Jain: Physiologically based pharmacokinetic modeling. Pinciples and applications. *J. Pharm. Sci.* **72**, 1103-1126 (1983).
17. P. H. Sonksen, J. R. McCormick, R. H. Egdahl, and J. S. Soeldner:

Distribution and binding of insulin in the dog hindlimb. *Am. J. Physiol.* 221, 1672-1680 (1971).

18. G. L. King and S. M. Johnson: Receptor-mediated transport of insulin across endothelial cells. *Science* **227**, 1583-1586 (1985).
19. S. I. Rapoport, W. A. Klee, K. D. Pettigrew, and K. Ohno: Entry of opioid peptides into the central nervous system. *Science* 207, 34-86 (1980).
20. R. R. Sharma and L. P. Vimal: Theoretical interpretation of extraction (in brain) of peptides including concentration variations. *Brain Res.* **308**, 201-214 (1984).
21. H. Sato, Y. Sugiyama, Y. Sawada, T. Iga, and M. Hanano: Binding of radioiodinated human β-endorphin to serum proteins from rats and humans, determined by several methods. *Life Sci.* **37**, 1309-1318 (1985).
22. H. S. G. Chen and J. F. Gross: Estimation of tissue-to plasma partition coefficients used in physiological pharmacokinetic models. *J. Pharmacokin. Biopharm.* **7**, 117-125 (1979).
23. R. J. Lutz, R. L. Dedrick, and D. S. Zaharko: Physiological pharmacokinetics. An in vitro approach to membrane transport. Pharmacol. Ther. 11, 559-592 (1980).
24. K. Yamaoka, Y. Tanigawara, T. Nakagawa, and T. Uno: A pharmacokinetic analysis program (MULTI) for microcomputer. *J. Pharmacobio-Dyn.* **4**, 879-885 (1981).
25. K. S. Pang and M. Rowland: Hepatic clearance of drugs. I. Theoretical consideration of a "well-stirred" model and a "parallel tube" model. Influence of hepatic blood flow, plasma and cell binding, and the hepatocellular enzymatic activity on hepatic drug clearence. *J. Pharmacokin. Biopharm.* **5**, 625-653

(1977).

26. K. Higaki and M. Fujimoto: Inulin carboxyl-^{14}C and ^{36}Cl spaces of various tissues of the rat. *J. Physiol. Soc. Jpn.* **31**, 164-172 (1969).
27. M. Gibaldi and D. Perrier. "Pharmacokinetics," 2nd Ed., pp. 45-111. Marcel Dekker, New York, 1982.
28. A. M. Hudson and C. McMartin: Mechanisms of catabolism of corticotrophin-(1-24)-tetracosapeptide in the rat in vivo. *J. Endocrinol.* **85**, 93-103 (1980).
29. F. A. Carone and R. P. Darryl: Hydrolysis and transport of small peptides by the proximal tubule. *Am. J. Physiol.* **238**, F151-F158 (1980).
30. J. R. Gillette and K. S. Pang: Theoretic aspects of pharmacokinetic drug interactions. *Clin. Phrmacol. Ther.* 22, 623-639 (1977).
31. C. A. Goresky, G. G. Bach, and C. P. Rose: Effects of saturating metabolic uptake on space profiles and tracer kinetics. *Am. J. Physiol.* **244**, G215-G232 (1983).
32. H. Sato, Y. Sugiyama, S. Miyauchi, Y. Sawada, T. Iga, and M. Hanano: A simulation study on the effect of a uniform diffusional barrier across hepatocytes on drug metabolism by evenly or unevenly distributed uni-enzyme in the liver. *J. Pharm. Sci.* **75**, 3-8 (1986).
33. L. E. Wittmers. M. Bartlett, and J. A. Johnson: Estimation of the capillary permeability coefficients of inulin in various tissues of the rabbit. *Microvasc. Res.* **11**, 67-78 (1976).
34. N. Ito, Y. Sawada, Y. Sugiyama, T. Iga, and M. Hanano:

Permeability of materials in postglomerular capillary bed and distribution to interstitium of kidney in rats. *Jpn. J. Physiol.* 35, 291-299 (1985).

35. L. J. Nugen and R. K. Jain: Plasma pharmacokinetics and interstitial diffusion of macromolecules in a capillary bed. *Am. J. Physiol.* 246, H129-H137 (1984).

36. W. P. Paaske: Microvascular exchange of albumin. *Microvasc. Res.* 25, 101-107 (1983).

37. C. A. Goresky, P. M. Huet, and J. P. Villeneuve: Blood-tissue exchange and blood flow in the liver. In "Hepatology: A Textbook of Liver Disease" (D. Zakim and T. Boyer, eds.), pp. 32-63. W. B. Saunders Co., Philadelphia, 1982.

38. E. Wisse, R. De Zanger, K. Charels, P. V. D. Smissen, and R. S. McCuskey: The liver sieve. Cosiderations concerning the structure and function of endothelial fenestrae, the sinusoidal wall, and the space of Disse. *Hepatology (Baltimore)* 5, 683-692 (1985).

39. P. J. McNamara, M. Gibaldi, and K. Stoeckel: Fraction unbound in interstitial fluid. *J. Pharm. Sci.* 72, 834-836 (1983).

40. H. P. J. Bennet and C. McMartin: Peptide hormones and their analogues. Distribution, clearance from the circulation, and inactivation in vivo. *Pharmacol. Rev.* 30, 247-292 (1979).

APPENDIX I: NOMENCLATURE

General

Q	= blood flow rate (ml/min)
V	= volume (ml)
C	= concentration of the drug (% dose/ml)
X	= amount of the drug (% dose)
t	= time after intravenous injection (min)
f	= unbound fraction of the drug
VR	= the volume ratio of ISF to the whole tissue
GFR	= glomerular fitration rate (ml/min)
kd	= degradation rate constant in renal tubules (% dose/min)
P	= transcapillary diffusion clearance (ml/min)
CL	= blood clearance (ml/min)
CL_{int}	= metabolic intrinsic clearance (ml/min)
CL_{influx}	= influx blood clearance (ml/min)
Kp	= tissue-to-blood partition coefficient
Kp^{*}	= interstitial fluid-to-blood partition coefficient
Rb	= blood-to-plasma partition coefficient
λ_z	= exponential slope of a terminal phase after intravenous injection (min^{-1})
τ	= time during the terminal phase after iv injection (min)
$I(t)$	= dose input function (% dose/min)
θ	= injection duration (min)
iv	= intravenous
ISF	= interstitial fluid

Subscripts

i	= i-type tissue
a	= arterial blood
v	= venous blood
p	= plasma (or serum)
app	= apparent
ss	= steady-state
u	= unbound
b	= bound
tot	= total
T	= whole tissue (excluding capillary bed)
B	= capillary bed or blood
IS	= interstitial fluid
IC	= intracellular water
H	= liver
R	= kidney
LU	= lung
HE	= heart
MU	= muscle
SK	= skin
GU	= gut
BR	= brain
AD	= adipose
RT	= renal tubules
U	= urine

APPENDIX II: EQUATIONS TO ESTIMATE TISSUE-TO-BLOOD PARTITION COEFFICIENTS

Case 1: For organs except the kidney, liver and lung

The differential equations describing the concentrations of the peptide hormone in the capillary bed and interstitial fluid are given by eqs. 5 and 6 in Materials and Methods. When the peptide is administered by intravenous bolus injection, the concentrations in each compartment will reach the terminal phase with an exponential slope of λ_z, when the concentrations in arterial blood, capillary bed and ISF are expressed as:

$$C_a = C_a^\tau e^{-\lambda_z(t-\tau)} \quad (A1)$$

$$C_B = C_{Bi}^\tau e^{-\lambda_z(t-\tau)} \quad (A2)$$

$$C_{IS} = C_{ISi}^\tau e^{-\lambda_z(t-\tau)} \quad (A3)$$

where C_a^τ, C_{Bi}^τ and C_{ISi}^τ are the concentrations in arterial blood, capillary bed and ISF at time τ during the terminal phase. Substituting for C_a^τ, C_{Bi}^τ and C_{ISi}^τ in eqs. 5 and 6 (in the text) according to eqs. A1-A3 and division by $e^{-\lambda_z(t-\tau)}$ yields:

$$-\lambda_z V_{Bi} C_{Bi}^\tau = Q_i(C_a^\tau - C_{Bi}^\tau) - P_i f_B(C_{Bi}^\tau - C_{ISi}^\tau/Kp_i^*) \quad (A4)$$

$$-\lambda_z V_{ISi} C_{ISi}^\tau = P_i f_B(C_{Bi}^\tau - C_{ISi}^\tau/Kp_i^*) - f_B CL_{int\,i} C_{ISi}^\tau/Kp_i^* \quad (A5)$$

Solving eq. A4 for C_{Bi}^τ gives:

$$C_{Bi}^\tau = \frac{Q_i C_a^\tau + P_i f_B C_{ISi}^\tau/Kp_i^*}{Q_i + P_i f_B - \lambda_z V_{ISi}} \quad (A6)$$

The interstitial fluid-to-arterial blood concentration ratio ($Kp_{i\,app}^*$) at the terminal phase is defined as:

$$Kp_{i\,app}^* = C_{ISi}^\tau/C_a^\tau \quad (A7)$$

Substituting for C_{Bi}^τ in eq. A4 according to eq. A6 and rearrangement using eq. A7 yields:

$$Kp^{*}_{i} = \frac{\left\{\frac{P_i f_B (Q_i - \lambda_z V_{Bi})}{Q_i + P_i f_B - \lambda_z V_{Bi}} + f_B CL_{int\,i}\right\} Kp^{*}_{i\,app}}{\frac{P_i Q_i f_B}{Q_i + P_i f_B - \lambda_z V_{Bi}} + \lambda_z V_{ISi} Kp^{*}_{i\,app}} \qquad (A8)$$

For non-eliminationg organs ($CL_{int\,i} = 0$), eq. A8 becomes:

$$Kp^{*}_{i} = \frac{\frac{P_i f_B (Q_i - \lambda_z V_{Bi})}{Q_i + P_i f_B - \lambda_z V_{Bi}} Kp^{*}_{i\,app}}{\frac{P_i Q_i f_B}{Q_i + P_i f_B - \lambda_z V_{Bi}} + \lambda_z V_{ISi} Kp^{*}_{i\,app}} \qquad (A9)$$

When $P_i f_B \gg Q_i$, i.e., in a blood flow-limited case, eqs. A8 and A9 simplify to the following equations, respectively:

$$Kp^{*}_{i} = \frac{(Q_i - \lambda_z V_{Bi} + f_B CL_{int\,i}) Kp^{*}_{i\,app}}{Q_i + \lambda_z V_{ISi} Kp^{*}_{i\,app}} \qquad (A10)$$

$$Kp^{*}_{i} = \frac{(Q_i - \lambda_z V_{Bi}) Kp^{*}_{i\,app}}{Q_i + \lambda_z V_{ISi} Kp^{*}_{i\,app}} \qquad (A11)$$

If $\lambda_z V_{Bi} \ll Q_i$, then eqs. A10 and A11 reduce to the equations derived by Chen and Gross (22) assuming a blood flow-limited model.

Case 2: For the kidney

The mass balance differential equations for the kidney are given by eqs. 12-15 (in the text), assuming that the renal clearance is attributable solely to the glomerular filtration with no reabsorption by the renal tubules. The last term of eq. 14, dX_U/dt, was neglected, because the excretion of ^{125}I-ß-EP in urine was small enough as compared with GFR and kd. During the terminal phase with an exponential slope of λ_z, the concentrations or amount of ^{125}I-ß-EP in the capillary bed, ISF, renal tubules and whole kidney tissue at time

are expressed by the equations similar to eqs. A1-A3. Therefore, according to eqs. 12-15, we obtain:

$$-\lambda_z V_{B,R} C^{\tau}_{B,R} = Q_R (C^{\tau}_a - C^{\tau}_{B,R}) - f_B GFR \cdot C^{\tau}_a - P_R f_B (C^{\tau}_{B,R} - C^{\tau}_{IS,R}/Kp^{*}_R) \qquad (A12)$$

$$-\lambda_z V_{IS,R} C^{\tau}_{IS,R} = P_R f_B (C^{\tau}_{B,R} - C^{\tau}_{IS,R}/Kp^{*}_R) \qquad (A13)$$

$$-\lambda_z X^{\tau}_{RT} = f_B GFR\, C^{\tau}_a - kd X^{\tau}_{RT} \qquad (A14)$$

$$V_{T,R} C^{\tau}_{T,R} = V_{IS,R} C^{\tau}_{IS,R} + X^{\tau}_{RT} \qquad (A15)$$

Substitution of $C^{\tau}_{B,R}$ in eq. 12 according to eq. A13 and rearrangement yields:

$$C^{\tau}_{IS,R} = \frac{\frac{P_R Q_R f_B (Q_R - f_B GFR)}{Q_R + P_R f_B - \lambda_z V_{B,R}} Kp^{*}_R C^{\tau}_a}{\frac{P_R f_B (Q_R - \lambda_z V_{B,R})}{Q_R + P_R f_B - \lambda_z V_{B,R}} - \lambda_z V_{IS,R} Kp^{*}_R} \qquad (A16)$$

Substituting for X^{τ}_{RT} and $C^{\tau}_{IS,R}$ in eq. A15 according to eqs. A14 and A16, respectively, and rearrangement yields:

$$Kp^{*}_R = \frac{\alpha V_{T,R} (Kp_{R,app} - \gamma)}{V_{IS,R}\{\beta + \lambda_z V_{T,R} (Kp_{R,app} - \gamma)\}} \qquad (A17)$$

where α, β and γ are expressed as:

$$\alpha = P_R f_B (Q_R - \lambda_z V_{B,R})/(Q_R + P_R f_B - \lambda_z V_{B,R}) \qquad (A18)$$

$$\beta = P_R f_B (Q_R - f_B GFR)/(Q_R + P_R f_B - \lambda_z V_{B,R}) \qquad (A19)$$

$$\gamma = f_B GFR/V_{T,R}/(kd - \lambda_z) \qquad (A20)$$

Case 3: For the liver

The mass-balance differential equation for the liver is written as follows, assuming a blood flow-limited model.

$$V_{IS,H}(dC_{IS,H}/dt) = (Q_H - Q_{GU})C_a + Q_{GU} C_{B,GU} - Q_H C_{IS,H}/Kp^{*}_H + f_B CL_{int,H} C_{IS,H}/Kp^{*}_H \qquad (A21)$$

Utilization of eqs. A1-A3 into eq. A21, solving for $C^{\tau}_{IS,H}$ and rearragement using eq. A7 finally gives:

$$Kp^{*}_{H} = \frac{(Q_H + f_B CL_{int,H})Kp^{*}_{H,app}}{Q_H - Q_{GU} + Q_{GU}\delta + \lambda_z V_{IS,H} Kp^{*}_{H,app}} \quad (A22)$$

where δ is given as:

$$\delta = (Q_{GU} + \lambda_z V_{IS,GU} Kp^{*}_{GU,app})/(Q_{GU} - \lambda_z V_{B,GU}) \quad (A23)$$

Case 4: For the lung

The mass-balance differential equations describing the concentrations in each compartment in the lung are given as follows:

$$V_a(dC_a/dt) = Q_{tot}(C_{B,LU} - C_a) \quad (A24)$$

$$V_{IS,LU}(dC_{IS,LU}/dt) = P_{LU} f_B (C_{B,LU} - C_{IS,LU}/Kp^{*}_{LU}) \quad (A25)$$

where V_a is the volume of the arterial blood and Q_{tot} is the total blood flow rate. Similar handling of the equations to Case 1 finally gives:

$$Kp^{*}_{LU} = \frac{P_{LU} f_B Kp^{*}_{LU,app}}{\frac{P_{LU} f_B (Q_{tot} - \lambda_z V_a)}{Q_{tot}} + \lambda_z V_{IS,LU} Kp^{*}_{LU,app}} \quad (A26)$$

If P_{LU} is very large and the first term of the denominator is much larger than the second term in eq. A26, then Kp^{*}_{LU} is expressed as:

$$Kp^{*}_{LU} = Q_{tot} Kp^{*}_{LU,app}/(Q_{tot} - \lambda_z V_a) \quad (A27)$$

In order to estimate the tissue-to-blood partition coefficient (Kp_i) for each tissue, we used the equations in which $V_{IS}i$ and $Kp^{*}_{i\,app}$ were converted to V_{Ti} and $Kp_{i\,app}$ by eqs. 8 and 9, respectively.

APPENDIX III: MODEL EQUATIONS FOR HUMAN ^{125}I-β-ENDORPHIN

Arterial blood:

$$V_a(dC_a/dt) = Q_{tot}(C_{B,LU} - C_a) \quad (A28)$$

Venous blood:

$$V_v(dC_v/dt) = Q_{HE}C_{B,HE} + Q_{MU}C_{B,MU} + Q_{SK}C_{B,SK} + Q_H C_{B,H} + Q_R C_{B,R} + Q_{BR}C_{B,BR} + Q_{AD}C_{B,AD} - Q_{tot}C_v + I(t) \quad (A29)$$

I(t) is the injection function proposed by Bischoff and Dedrick (11) and expressed as:

$$I(t) = 30 \cdot Dose/\theta (t/\theta)^2 (1 - t/\theta)^2 \quad (A30)$$

where θ is the injection duration (minutes).

Lung:

$$V_{B,LU}(dC_{B,LU}/dt) = Q_{tot}(C_v - C_{B,LU}) - P_{LU} f_B (C_{B,LU} - C_{T,LU}/Kp_{LU}) \quad (A31)$$

$$V_{T,LU}(dC_{T,LU}/dt) = P_{LU} f_B (C_{B,LU} - C_{T,LU}/Kp_{LU}) \quad (A32)$$

Heart:

$$V_{B,HE}(dC_{B,HE}/dt) = Q_{HE}(C_a - C_{B,HE}) - P_{HE} f_B (C_{B,HE} - C_{T,HE}/Kp_{HE}) \quad (A33)$$

$$V_{T,HE}(dC_{T,HE}/dt) = P_{HE} f_B (C_{B,HE} - C_{T,HE}/Kp_{HE}) \quad (A34)$$

Muscle:

$$V_{B,MU}(dC_{B,MU}/dt) = Q_{MU}(C_a - C_{B,MU}) - P_{MU} f_B (C_{B,MU} - C_{T,MU}/Kp_{MU}) \quad (A35)$$

$$V_{T,MU}(dC_{T,MU}/dt) = P_{MU} f_B (C_{B,MU} - C_{T,MU}/Kp_{MU}) \quad (A36)$$

Skin:

$$V_{B,SK}(dC_{B,SK}/dt) = Q_{SK}(C_a - C_{B,SK}) - P_{SK} f_B (C_{B,SK} - C_{T,SK}/Kp_{SK}) \quad (A37)$$

$$V_{T,SK}(dC_{T,SK}/dt) = P_{SK} f_B (C_{B,SK} - C_{T,SK}/Kp_{SK}) \quad (A38)$$

Liver:

$$V_{T,H}(dC_{T,H}/dt) = (Q_H - Q_{GU})C_a + Q_{GU}C_{B,GU} - Q_H C_{T,H}/Kp_H + f_B CL_{int,H} C_{T,H}/Kp_H \quad (A39)$$

Gut:

$$V_{B,GU}(dC_{B,GU}/dt) = Q_{GU}(C_a - C_{B,GU}) - P_{GU}f_B(C_{B,GU} - C_{T,GU}/Kp_{GU}) \quad (A40)$$

$$V_{T,GU}(dC_{T,GU}/dt) = P_{GU}f_B(C_{B,GU} - C_{T,GU}/Kp_{GU}) \quad (A41)$$

Kidney:

$$V_{B,R}(dC_{B,R}/dt) = Q_R(C_a - C_{B,R}) - f_B GFR \cdot C_a - P_R f_B(C_{B,R} - C_{IS,R}/Kp^*_R) \quad (A42)$$

$$V_{IS,R}(dC_{IS,R}/dt) = P_R f_B(C_{B,R} - C_{IS,R}/Kp^*_R) \quad (A43)$$

$$dX_{RT}/dt = f_B GFR \cdot C_a - kdX_{RT} \quad (A44)$$

$$V_{T,R}C_{T,R} = V_{IS,R}C_{IS,R} + X_{RT} \quad (A45)$$

Brain:

$$V_{B,BR}(dC_{B,BR}/dt) = Q_{BR}(C'_a - C_{B,BR}) - P_{BR}f_B(C_{B,BR} - C_{T,BR}/Kp_{BR}) \quad (A46)$$

$$V_{T,BR}(dC_{T,BR}/dt) = P_{BR}f_B(C_{B,BR} - C_{T,BR}/Kp_{BR}) \quad (A47)$$

Adipose:

$$V_{B,AD}(dC_{B,AD}/dt) = Q_{AD}(C_a - C_{B,AD}) - P_{AD}f_B(C_{B,AD} - C_{T,AD}/Kp_{AD}) \quad (A48)$$

$$V_{T,AD}(dC_{T,AD}/dt) = P_{AD}f_B(C_{B,AD} - C_{T,AD}/Kp_{AD}) \quad (A49)$$

Table I. Pharmacokinetic Parameters of Human ^{125}I-β-Endorphin in a 240-g Rat

Dose	A^a (% dose/ml)	α^a (min^{-1})	B^a (% dose/ml)	β^a (min^{-1})	$V_1{}^b$ (ml)	$Vd_{ss}{}^c$ (ml)	$CL_{tot}{}^d$ (ml/min)
Tracer	1.46[e]	0.331	0.238	0.0294	14.2	40.3	2.95
	± 0.08	± 0.064	± 0.081	± 0.0038	± 0.6	± 0.6	± 1.01
Tracer plus	1.65[e]	0.370	0.261	0.0466	12.9	34.8	3.25
168 μg/kg β-EP	± 0.23	± 0.116	± 0.052	± 0.0246	± 1.6	± 4.6	± 1.48
Recovered	0.725[g]	0.334	0.441	0.0576	20.6	34.6	3.35
parameters[f]	± 0.073	± 0.057	± 0.047	± 0.0039	± 2.0	± 7.1	± 0.73
	(50 %)[h]	(101 %)	(169 %)	(124 %)	(145 %)	(86 %)	(113 %)

[a] Calculated by a non-linear least squares regression (24). $C_p = Ae^{-\alpha t} + Be^{-\beta t}$.

[b] Calculated as V_1 = Dose/(A + B), where the dose is 24 (% dose) for a 240-g rat.

[c] Calculated as $Vd_{ss} = Dose(A\beta^2 + B\alpha^2)/(A\beta + B\alpha)^2$.

[d] Calculated as CL_{tot} = Dose/$(A/\alpha + B/\beta)/R_B$, where R_B is 0.82.

[e] Each value is expressed as the mean ± SE of three rats.

[f] Obtained by fitting the five simulated points (2, 5, 15, 30 and 60 min) of plasma concentration of ^{125}I-β-EP to a biexponential equation, $C_p = Ae^{-\alpha t} + Be^{-\beta t}$.

[g] Each value is the mean ± SD of the estimated parameter.

[h] Numbers in parentheses mean the percent recovered from the original values.

Table II. Physiological Constants and Parameters for a 240-g Rat Used in the Simulation of Distribution and Elimination of Human ^{125}I-β-Endorphin

Tissue	Tissue volume, V_T (ml)[a]	Capillary bed volume, V_B (ml)[a]	Interstitial space, VR (%)[a]	Blood flow, Q (ml/min)[a]	Kp_{app}[e]	P[f] (ml/min)	Kp[g]
Venous blood	2.9	2.9		35.2			
Arterial blood	1.5	1.5		35.2			
Lung	1.6	0.6	19	35.2	0.79 ± 0.18	0.13	0.44
Heart	1.0	0.4	10	1.5	0.18 ± 0.01	0.079	0.16
Muscle	108.0	1.4	12	6.5	0.10 ± 0.02	2.2	0.079
Skin	43.0	0.4	30	4.4	0.65 ± 0.17	0.41	0.15
Liver	8.0	2.0	16	6.7	0.37 ± 0.03	-[h]	0.51
Gut	16.0	6.0	9.4	4.7	0.23 ± 0.10	1.4	0.19
Kidney	2.0	5.0	20	13.3	2.2 ± 0.22	4.5	0.67
Brain	1.2	0.013[c]	0.4[d]	1.1	0.038 ± 0.005	0.0035	0.024
Adipose	9.6[b]	0.069	14	1.7[b]	0.095 ± 0.019	0.035	0.044

[a] Taken or calculated from ref. 15 except for the brain and adipose.

[b] Taken from ref. 14.

[c] Calculated from ref. 13.

[d] Taken from ref 27.

[e] Tissue-to-arterial blood concentration ratios determined 60 min after iv bolus injection. Each value is expressed as the mean ± SE of three rats.

[f] Transcapillary diffusion clearances estimated by curve fitting using a hybrid model (23).

[g] Tissue-to-blood partition coefficients corrected from Kp_{app} using equations in Appendix II. The value of $\overset{*}{Kp}$ multiplied by VR (0.2) is listed for the kidney.

[h] Blood flow-limited distribution of ^{125}I-β-EP is assumed for the liver.

Table III. Recovered Pharmacokinetic Parameters of Human ^{125}I-β-Endorphin in a 240-g Rat, Obtained from the Points Simulated Using the Two One-organ Models[a]

One-organ Models	A[b] (% dose/ml)	α[b] (min^{-1})	B[b] (% dose/ml)	β[b] (min^{-1})	V_1[c] (ml)	Vd_{ss}[c] (ml)	CL_{tot}[c] (ml/min)
Blood flow-limited Model	0.326[d] ± 0.010 (22.3 %)[e]	0.418 ± 0.017 (126 %)	0.256 ± 0.003 (108 %)	0.0364 ± 0.0004 (124 %)	41.2 ± 0.90 (290 %)	76.7 ± 1.9 (190 %)	3.07 ± 0.12 (104 %)
Diffusion-limited Model	0.725[d] ± 0.073 (50 %)	0.334 ± 0.057 (101 %)	0.441 ± 0.047 (169 %)	0.0576 ± 0.0039 (124 %)	20.6 ± 2.0 (145 %)	34.6 ± 7.1 (86 %)	3.35 ± 0.73 (113 %)

[a] Simulations were performed using a physiologically based pharmacokinetic model assuming either the blood flow-limited or capillary membrane-limited distribution of ^{125}I-β-EP from the blood to ISF in a one-organ model.

[b] Obtained by fitting the five simulated points (2, 5, 15, 30 and 60 min) of plasma concentration of ^{125}I-β-EP to a biexponential equation, $C_p = Ae^{-\alpha t} + Be^{-\beta t}$.

[c] Calculated as in Table I.

[d] Each value is the mean ± SD of the estimated parameter.

[e] Numbers in parentheses mean the percent recovered from the original values.

FIGURE LEGENDS

Fig. 1. *Schematic diagram of a physiologically based pharmacokinetic model for ^{125}I-β-EP in rats.*

Fig. 2. *Schematic representation of a one-organ model for an eliminating organ subdivided anatomically into the three fluid compartments.*

Fig. 3. *Representative get filtration profiles of ^{125}I-β-EP on Sephadex G-50 from rat plasma.*

Serum was obtained at designated times after iv bolus injection of ^{125}I-β-EP (8 μCi/kg) with (below) and without (above) 168 μg/kg of unlabeled β-EP in rats and chromatographed on a Sephadex G-50 column (1 x 45 cm) equilibrated and eluted with 20% v/v acetic acid containing 0.01 M ammonium acetate.

Fig. 4. *Representative gel filtration profiles of ^{125}I-β-EP on Sephadex G-50 from rat urine and bile.*

Urine and bile were collected 0-10 and 90-180 min after iv bolus injection of ^{125}I-β-EP (8 μCi/kg), respectively, and chromatographed on a Sephadex G-50 column (1 X 45 cm) equilibrated and eluted with 20% v/v acetic acid containing 0.01 M ammonium acetate.

Fig. 5. *Time or concentration vs. blood-to-plasma partition coefficient (R_B) of ^{125}I-β-EP in vitro.*

^{125}I-β-EP was incubated in pooled rat blood at 37 °C, and the change in the R_a value of ^{125}I-β-EP was examined with time (panel A) and concentration (panel B). See the text for details.

Fig. 6. *Relationship between the transcapillary diffusion clearances (P) of inulin and those of ^{125}I-β-EP for various tissues in rats.*

The P values of ^{125}I-β-EP were determined by a nonlinear least squares regression analysis of the concentration profiles of ^{125}I-β-EP in various tissues using a hybrid model (23). The P values of inulin were cited from ref. 15. The regression line is $y = 1.07x - 0.26$ ($r = 0.986$, $p < 0.005$).

Fig. 7. *Simulated curves and observed ^{125}I-β-EP for concentrations in plasma and in various tissues after iv bolus injection in rats.*

The concentration (% dose/ml) of ^{125}I-β-EP in plasma and in various tissues were examined at designated times after the iv injection of tracer doses of ^{125}I-β-EP (approximately 8 μg/kg) in rats. Each point and vertical bar represent the mean and SE of three individual rats. Solid lines show the simulated curves based on the physiological pharmacokinetic model incorporating the transcapillary diffisional barrier for ^{125}I-β-EP.

Fig. 8. *Difference in the simulated plasma concentrations of ^{125}I-β-EP between the two physiologically based pharmacokinetic models in rats.*

Each point and vertical bar represent the mean and SE of the observed plasma concentrations (% dose/ml) of ^{125}I-β-EP after iv injection in three individual rats. Solid and broken lines are the simulated curves by the capillary membrane-limited and the blood flow-limited models, respectively. See text for details.

Fig. 1

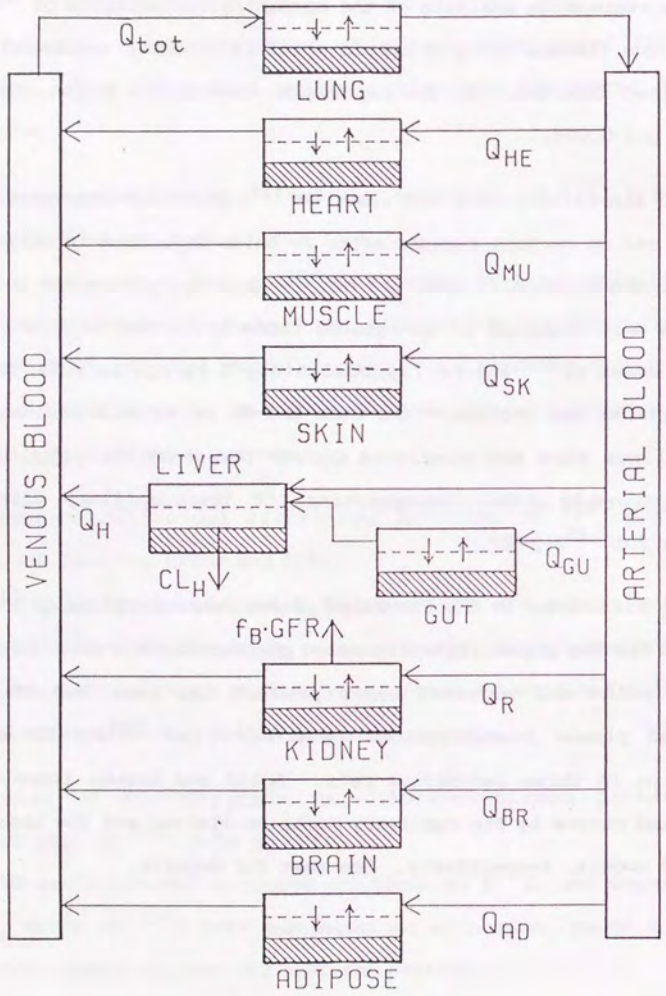
Q_{tot}
LUNG
Q_{HE}
HEART
Q_{MU}
MUSCLE
Q_{SK}
SKIN
LIVER
Q_H
CL_H
Q_{GU}
GUT
$f_B \cdot GFR$
Q_R
KIDNEY
Q_{BR}
BRAIN
Q_{AD}
ADIPOSE
VENOUS BLOOD
ARTERIAL BLOOD

Fig. 2

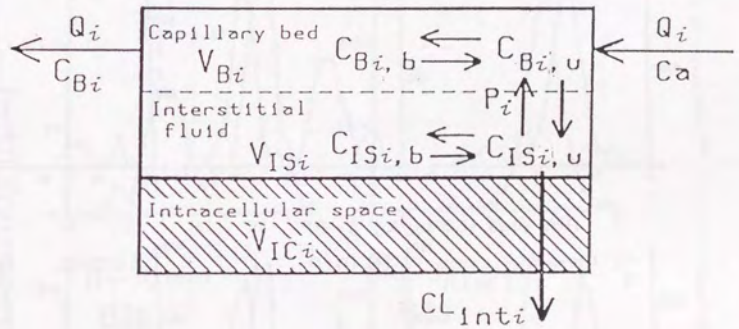
Q_i
C_{Bi}
Capillary bed
V_{Bi}
$C_{Bi,b}$
$C_{Bi,u}$
Q_i
Ca
P_i
Interstitial fluid
V_{ISi}
$C_{ISi,b}$
$C_{ISi,u}$
Intracellular space
V_{ICi}
CL_{inti}

Fig. 3

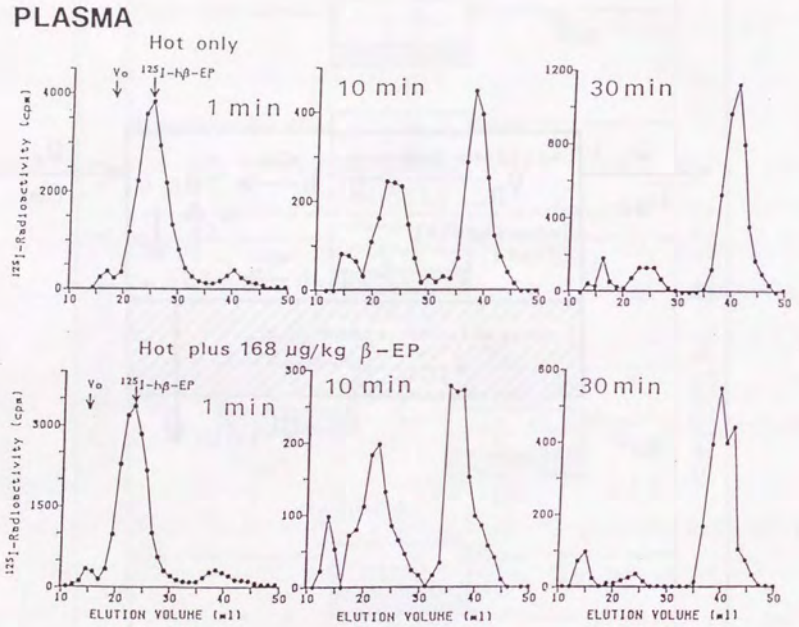
PLASMA
Hot only
Vo
125I-hβ-EP
1 min
10 min
30 min
125I-Radioactivity (cpm)
Hot plus 168 µg/kg β-EP
ELUTION VOLUME (ml)

Fig. 4

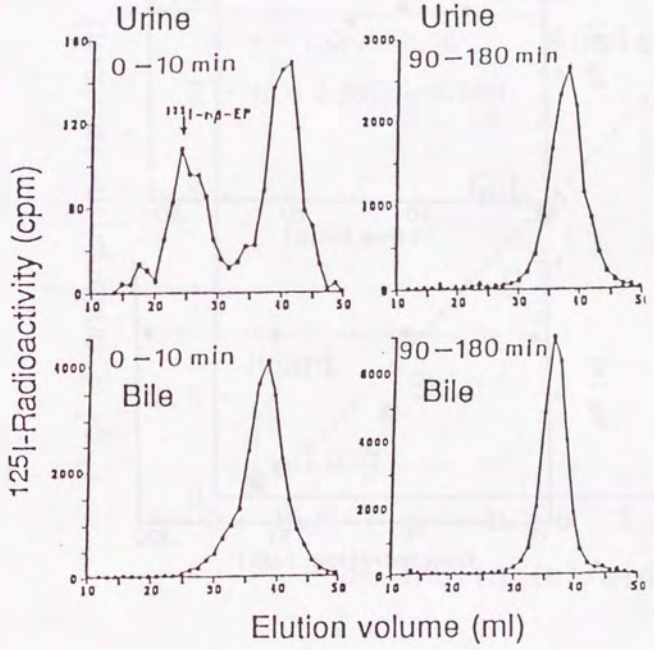
Urine
0 – 10 min
125I-hβ-EP
Urine
90 – 180 min
0 – 10 min
Bile
90 – 180 min
Bile
125I-Radioactivity (cpm)
Elution volume (ml)

Fig. 5

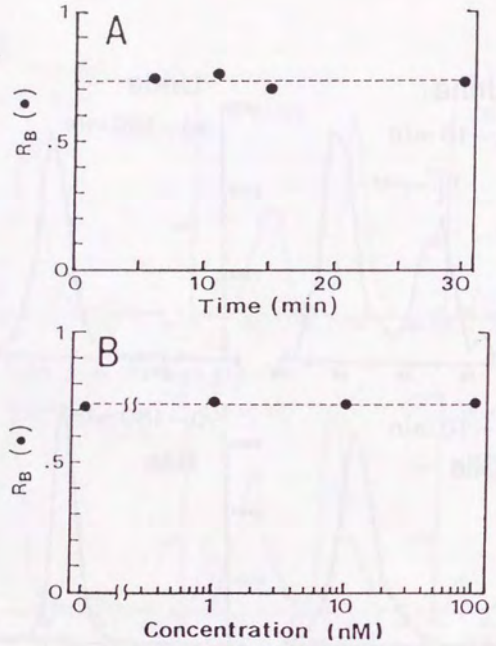
A
B
R_B (•)
1
.5
0
10
20
30
Time (min)
0
1
10
100
Concentration (nM)

Fig. 6

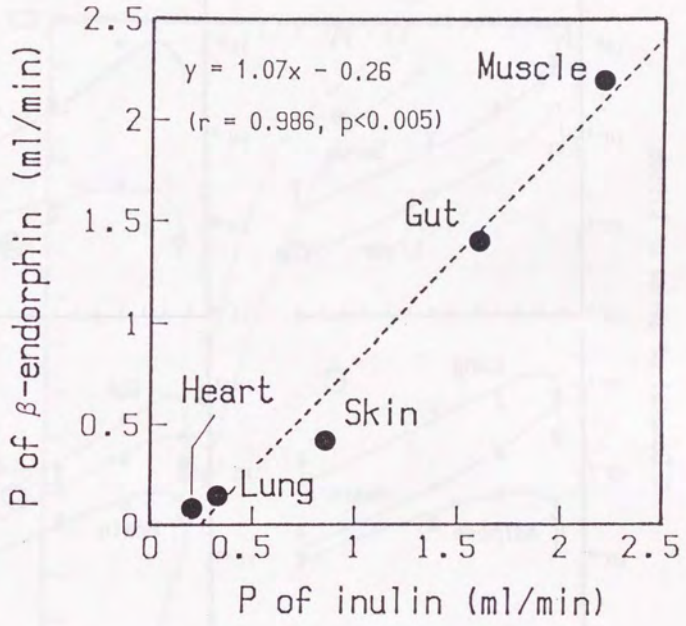
y = 1.07x - 0.26
(r = 0.986, p<0.005)
Muscle
Gut
Skin
Heart
Lung
P of β-endorphin (ml/min)
P of inulin (ml/min)
2.5
2
1.5
1
0.5
0
0.5
1
1.5
2
2.5

Fig. 7

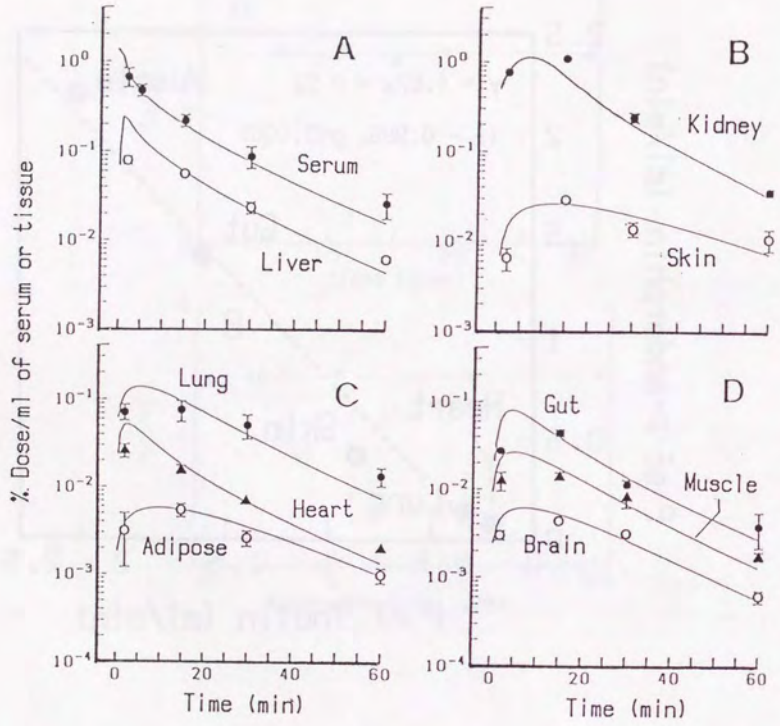
A
B
C
D
Serum
Liver
Kidney
Skin
Lung
Heart
Adipose
Gut
Muscle
Brain
% Dose/ml of serum or tissue
Time (min)
Time (min)

Fig. 8

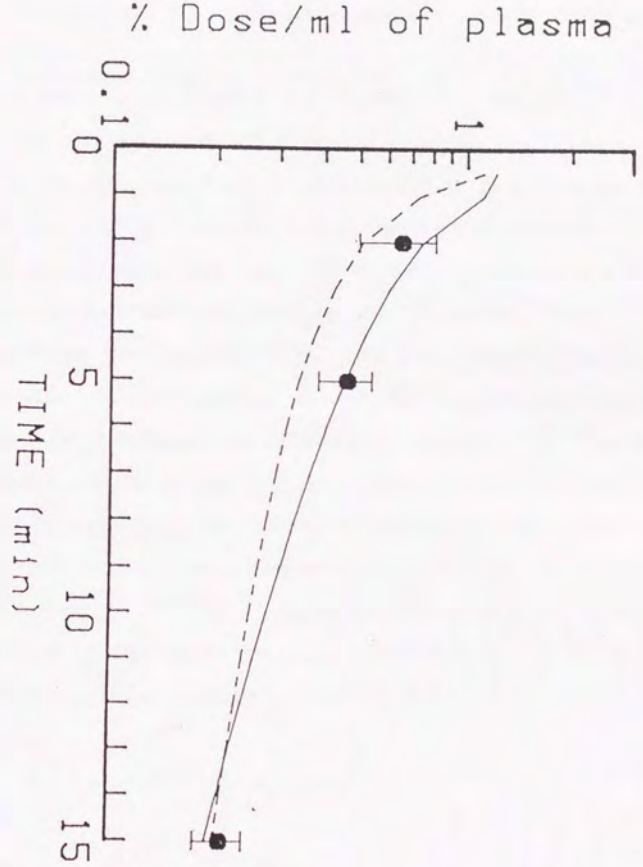
% Dose/ml of plasma
TIME (min)

PART II

IN VIVO EVIDENCE FOR THE SPECIFIC BINDING OF HUMAN β-ENDORPHIN TO THE LUNG AND LIVER OF THE RAT

SUMMARY

Specific binding of human β-endorphin (β-EP) was demonstrated in the lung and liver of the rat *in vivo* by the following lines of evidence using [^{125}I-Tyr^{27}]β-EP as a radiolabeled tracer. First, the tissue-to-serum concentration ratios of the intact labeled peptide 15 min after intravenous administration was significantly decreased in the lung and liver by a simultaneous injection of unlabeled β-EP (48.5 nmole/kg), whereas in the other tissues such a decrease was not observed. Second, serum concentrations of the preadministered labeled peptide was rapidly increased after additional intravenous injection *via* the femoral vein, but not *via* the carotid artery into the heart. Third, the immunoreactive labeled β-EP (^{125}I-β-EP), which was purified on a Sephadex G-50 column and did not specifically bind to the rat brain membranes, was neither accumulated in the lung and liver nor displaced by unlabeled β-EP *in vivo*, in contrast to [^{125}I-Tyr^{27}]β-EP, the commercially available HPLC-purified labeled peptide. Fourth, an additional injection of dynorphin-(1-13) or ethylketocyclazocine (kappa agonist) also increased the serum concentrations of preadministered [^{125}I-Tyr^{27}]β-EP, while that of D-Ala^{2}-D-Leu^{5}-enkephalin (delta agonist) nor naloxone (mu antagonist) did, suggesting the kappa-type binding sites in the lung.

INTRODUCTION

β-Endorphin (β-EP)[1] is a 31-residue endogenous peptide with potent opioid properties [1]. Since the specific binding sites of β-EP have been found not only in the brain but also in some peripheral tissues [2-5], increasing attention has been paid to the peripheral direct endorphin actions. On the other hand, in the field of pharmacokinetics, the important roles of the peripheral receptor binding in the distribution and metabolism of peptide hormones such as insulin [6-8] and arginine vasopressin [9] have been demonstrated. Recently, Whitcomb *et al.* [10] described a unique *in vivo* radioreceptor assay for the identification of tissue insulin receptors. In the present study, therefore, we used a similar method to examine the peripheral specific binding of [^{125}I-Tyr^{27}]β-EP which is commercially available, purified by high-performance liquid chromatogrphy and specifically binds to the opioid receptors in the brain. We also used an *in vivo* displacement technique to certify the specific binding of the labeled peptide to the lung. Moreover, we performed the above experiments using an unfractionated labeled β-EP (^{125}I-β-EP) which lacks the opioid receptor binding activity, in order to examine the effect of receptor binding activity on *in vivo* distribution of β-EP, by comparing the distribution characteristics between the two radioiodinated peptides.

MATERIALS AND METHODS

Bindings of Labeled β-Endorphins to Rat Brain Membranes. The rat brain membrane (RBM) fraction was prepared as previously described [11] and used for the receptor binding assay. Bindings of [^{125}I-Tyr^{27}]β-EP and ^{125}I-β-EP to RBM was carried out as follows. The membrane pellet was resuspended in ice-cold 50 mM Tris-HCl buffer (pH 7.4) containing 0.1 % bovine serum albumin, 3 mM $MgSO_4$, 500 KIU/ml Trasylol, 0.02 % bacitracin, 0.001 % leupeptin, and 0.001 % pepstatin to a concentration of 2.0 mg protein/ml (designated as the membrane solution). Labeled β-EP (10000 cpm) and varying concentrations of unlabeled human β-EP (0, 1, 4, 10, 40, 100, and 1000 nM) were added to 1.5 ml of the membrane solution and incubated at 0°C for 2 hr. Binding was terminated by centrifugation for 1 min in a Beckman tabletop microcentrifuge at 4°C and residual unbound ligand was rapidly removed by aspiration. The radioactivity was counted in supernatant and in precipitation, respectively, and the percent bound was defined as (cpm in precipitate)/[(cpm in supernatant) + (cpm in precipitate)] x 100. Each binding assay was performed in triplicate.

Tissue Distribution of the Labeled Peptides after Intravenous Injection. Adult male Wistar rats (Nihon Seibutsu Zairyo, Tokyo, Japan) weighing 240-280 g were used throughout the experiments. [^{125}I-Tyr^{27}]β-EP (4 μCi/kg) with or without unlabeled β-EP (48.5 nmole/kg) or only ^{125}I-β-EP (4 μCi/kg) was injected through the femoral vein. The rats were sacrificed by cutting the carotid artery at 15 min and the liver, kidney, lung, muscle, adipose (retroperitoneal fat), gut (first third of the small intestine), heart, brain, and skin were quickly excised, rinsed with ice-cold saline, blotted dry, and a portion of each tissue was weighed and

counted for the total radioactivity in a gamma-counter (model ARC-300, Aloka Co. Ltd., Tokyo, Japan) with a counting efficiency of approximately 80 %. Another portion (0.5 g) was quickly added to ice-cold 5 ml of 20 % acetic acid solution containing ammonium acetate (designated as AcOH solution) and stored at -40°C. Determination of the percent of trichloroacetic acid (TCA)-precipitable radioactivity in each tissue was performed as previously described [12]. Briefly, each tissue was homogenized in the AcOH solution in a motor-driven Potter homogenizer, 1 ml of the homogenate was added to 1 ml of 30 % TCA, mixed well, centrifuged, and TCA-precipitable radioactivity determined.

Additional Injection of Unlabeled β-EP or Selective Opioid Ligands after Labeled Tracer Injection. [^{125}I-Tyr^{27}]β-EP or ^{125}I-β-EP (4 μCi/kg) plus saline up to 200 μl was injected through the femoral vein in conscious rats, followed by an additional injection of unlabeled β-EP (48.5 nmole/kg) at 15 min. Unlabeled β-EP was also injected through the cannulated carotid artery into the heart, followed by an equal injection of saline, when [^{125}I-Tyr^{27}]β-EP was preadministered. Moreover, 48.5 nmole/kg of dynorpin (1-13) (DYN) or ethylketocyclazocin (EKC), 3.1 μmole/kg of naloxone, or 240 nmole/kg of D-Ala-D-Leu-enkephalin (DADLE) was intravenously injected at 15 min after i.v. injection of [^{125}I-Tyr^{27}]β-EP. In each above experiment, blood was withdrawn through the femoral artery at designated times, serum (50-200 μl) was added to 2 ml of 15 % TCA, and the subsequent procedure was the same as described above for tissue samples. Some samples were gel chromatographed on a Sephadex G-50 column (1 x 45 cm) eluted with the AcOH solution.

Data Calculations. TCA-precipitable radioactivity (cpm) was determined in serum or tissues as described above, and concentrations of the labeled β-EPs were expressed as the percent of the dose injected per ml serum or g tissue. For the tissues, the tissue-to-arterial serum concentration ratios (designated as Kp_{app}) 15 min after the tracer injection were calculated as (cpm/g tissue)/(cpm/ml serum).

Materials. [^{125}I-Tyr^{27}]β-EP obtained from the Radiochemical Center (Amersham, Arlington Heights, IL) was reportedly prepared by iodination of synthetic human β-EP using Na^{125}I and chloramine-T, and fractionated by HPLC. The unfractionated labeled human β-EP (^{125}I-β-EP) with a specific activity of 83 μCi/ug was prepared by the chloramine-T method and gel chromatography on Sephadex G-50 as previously described [13]. The labeled peptides (fractionated and unfractionated) were stored at -40°C until study. As assayed by chromatography on Sephadex G-50, these labeled tracers were at least 95 % pure within a month. Following N-terminal cleavage of these tracers by leucine aminopeptidase (0.2 mg/ml) at 37°C for 1 hr and the thin-layer chromatography of the digestion products eluted with butanol-1-ol/acetic acid/water (75:13:12 V/V) as previously described [14], approximately 30 % of the radioactivity appeared as monoiodotyrosine from the unfractionated tracer, while no radioactivity from the fractionated tracer. Therefore, the unfractionated tracer was found to be iodinated at Tyr^{1} as well as Tyr^{27}, while the fractionated tracer was labeled only at Tyr^{27}. DYN and EKC were kindly supplied from Eisai Co. (Tokyo, Japan). Naloxone and DADLE were purchased from Sigma Chemical Co. (St. Louis, MO), human β-EP and TCA from Wako Pure Chemical Industries, Ltd. (Osaka, Jpan) and Sephadex G-50 from Pharmacia Fine Chemical Co. (St. Luis,

MO). All other reagents were of analytical grade and commercially available without the need for further purification.

RESULTS

Bindings of Labeled β-EPs to RBM. Figure 1 shows the bindings of [^{125}I-Tyr^{27}]β-EP (fractionated by HPLC) and ^{125}I-β-EP (unfractionated) to RBM, inhibited by unlabeled β-EP. The specific and nonspecific bindings of [^{125}I-Tyr^{27}]β-EP was 16.5 % and 8.7 % of the labeled tracer added, respectively, while those of ^{125}I-β-EP was 1.1 % and 13.4 %, respectively, indicating that the unfractionated tracer retains little opioid receptor binding activity. The IC_{50} for [^{125}I-Tyr^{27}]β-EP binding was 4.9 nM and close the the previously reported value (3.5 nM) obtained by inhibition of ^{3}H-β-EP binding to RBM by unlabeled β-EP at 0°C [15]. Therefore, it follows that the fractionated labeled tracer is close to native human β-EP in its binding property, while the unfractionated tracer is not.

Tissue Distribution of the Labeled Peptides after Intravenous Injection. Table I shows the tissue-to-arterial serum concentration ratios (Kp_{app}) of [^{125}I-Tyr^{27}]β-EP with and without unlabeled β-EP and of ^{125}I-β-EP 15 min after the tracer injection *via* the femoral vein. The volume ratios of the interstitial fluid to the whole tissue (designated as IFV, the fractional interstitional vluid volume) in several tissues examined were cited from references [16,17] and included in Table I for the comparison with Kp_{app} of the labeled β-EPs. The tissues showing Kp_{app} of more than 1 for the fractionated and unfractionated tracers are liver, kidney, and lung, and only kidney, respectively, indicating that these tissues accumulated the respective peptide more than the serum concentration at pseudoequilibrium condition (terminal phase after i.v. injection). A significant decrease in the Kp_{app} values of the fractionated tracer by the simultaneous injection of unlabeled β-EP was observed for the lung

($p < 0.02$) and liver ($p < 0.05$). The Kp_{app} values of the unfractionated tracer and the fractionated tracer with the unlabeled β-EP were similar to the fractional IFV in each tissue except kidney.

Additional Injection of Unlabeled β-EP or Selective Opioid Ligands after Labeled Tracer Injection. Figure 2A presents the effect of an additional injection of unlabeled β-EP *via* the femoral vein or carotid artery on the serum disappearance of [^{125}I-Tyr^{27}]β-EP. There was an immediate increase in the serum concentration of [^{125}I-Tyr^{27}] β-EP by 153 ± 69 % (mean ± SE, n=3) 1 min after i.v. injection of unlabeled β-EP, while such an increase was not observed after the arterial injection. Figure 2B presents the effect of an additional injection of unlabeled β-EP *via* the femoral vein on the serum disappearance of ^{125}I-β-EP. Increase in serum concentrations of ^{125}I-β-EP was not observed in contrast to [^{125}I-Tyr^{27}]β-EP. As shown in Figs. 3A-3D, *in vivo* displacement of [^{125}I-Tyr^{27}]β-EP was demonstrated by an additional injection of DYN or EKC, but not by that of much larger amount of naloxone or DADLE.

DISCUSSION

There are two tyrosine residues in β-EP molecule to be iodinated, and the importance of the N-terminal tyrosine for its biological activity has been reported [18]. Moreover, Houghten *et al.* [19] reported that the presence of diiodotyrosine in position 1 and in positions 1 and 27 dramatically reduced the opiate activity (< 1 % of native β-EP), while diiodinated β-EP in position 27 still remains 37 % of the opiate activity. TLC after leucine aminopeptidase digestion showed that ^{125}I-β-EP was iodinated at Tyr^{1} and Tyr^{27}. Therefore, it is likely that nearly complete reduction of the receptor binding activity of ^{125}I-β-EP was resulted from the iodination of β-EP at the biologically active N-terminal tyrosine, while monoiodination of β-EP at Tyr^{27} did not change the receptor binding activity of β-EP. In the present study, therefore, the unfractionated tracer (^{125}I-β-EP) was used to examine the effect of receptor binding activity on the *in vivo* distribution of β-EP, by comparing the distribution characteristics between the two radioiodinated peptides.

We demonstrated in this study that [^{125}I-Tyr^{27}]β-EP specifically binds to the lung and liver of the rat by an *in vivo* radioreceptor assay technique [10] using the HPLC-fractionated and unfractionated labeled peptides as tracers. It was suggested that the saturable binding of [^{125}I-Tyr^{27}]β-EP to the lung and liver is related to the receptor binding activity, from the observations that the Kp_{app} values of the unfractionated tracer were similar to those of the fractionated tracer with unlabeled β-EP in each tissue except for the kidney and that ^{125}I-β-EP was not displaced by i.v. injection of unlabeled β-EP in contrast to [^{125}I-Tyr^{27}]β-EP. When [^{125}I-Tyr^{27}]β-EP was injected through the carotid artery, serum concentrations of the tracer

measured at the femoral artery were much higher than those of the intravenously injected tracer (result not shown), thus excluding the possibility that the arterially injected unlabeled β-EP was not efficiently mixed with circulating blood due to the arterial blood pressure. The tissue-to-serum partition coefficient (Kp), which represents the real concentration ratio of the tissue to serum at equilibrium condition, can be calculated from the Kp_{app} values based on the physiological model [20]. According to that theory, the tissue-to-arterial serum concentration ratio (Kp_{app}) obtained at pseudoequilibrium condition should be equal to or larger than Kp for noneliminating organs with large distributin volumes and less than Kp for eliminating organs such as liver and kidney. Such a correctin factor is identical in all experiments with and without simultaneous injection of unlabeled β-EP, and therefore the Kp_{app} values (not corrected to the Kp values) deserve an appropriate interpretation for the saturability of the distribution of labeled peptides into tissues, which is the purpose intended.

An intravenously (not arterially) administered substance is subject to the first pass through the lung before it reaches the systemic circulation. Therefore, it follows from *in vivo* displacement experiments (Fig. 2A) that the lung is responsible for the rapid dissociation of [^{125}I-Tyr^{27}]β-EP after intravenously injected unlabeled β-EP, suggesting that the binding site in the lung is located close to the pulmonary capillaries. Sapru *et al.* [21] showed that an enkephalin-analog stimulated the pulmonary J receptors (juxta-pulmonary capillary receptors) located at the alveolar level close the pulmonary capillaries. However, the present study provides a unique

in vivo evidence for the existence of peripheral specific binding site(s) of β-EP, since the interaction of β-EP with the lung has never been described elsewhere. Moreover, from *in vivo* displacement (washout) experiments using selective opioid ligands, it was suggested that the specific binding sites in the lung have a significant kappa-type property, although it is accepted that the affinity of β-EP to kappa sites is not so high as to mu or delta sites in the central nervous system. The lung was shown to play an important role in the distribution of β-EP as a depot when the serum concentrations are monitored in the artery (except for the pulmonary artery) after the additional i.v. injection of unlabeled β-EP, because the blood in the artery (emerging from the lung) is in equilibrium with the pulmonary tissue. Similarly, in order to examine the dissociation of the labeled peptide from the liver by unlabeled peptide, we should measure the concentrations of the labeled peptide in hepatic vein (emerging from the liver) after the additional i.v. injection of unlabeled peptide.

That [^{125}I-Tyr^{27}]β-EP showed specific binding to the rat liver corresponds to the recent observation by Dave *et al.* [2] in which ^{125}I-labeled acetyl-human β-endorphin (Ac-hBE) was used as a tracer. Dave *et al.* also observed the specific binding of Ac-hBE to the kidney, adrenal, spleen, and testis of the rat using isolated membrane preparations. Although the decrease in Kp_{app} was observed in the kidney (Table I), our *in vivo* radioreceptor assay could not significantly detect the specific binding of [^{125}I-Tyr^{27}]β-EP, mainly due to the relatively large nonspecific binding of the peptide in the kidney (Kp = 3.50, determined at the i.v. dose of 48.5 nmole/kg) in contrast to the liver and lung. Such a large nonspecific retention in

the kidney may be related to the physiological renal functions (i.e., the glomerular filtration and retention in the tubules, followed by peptidase digestion) maintained in the intact organism.

In conclusion, peripheral specific binding of human β-EP was demonstrated in the lung and liver of the rat by an *in vivo* radioreceptor assay using [^{125}I-Tyr^{27}]β-EP as a radiolabeled tracer. *In vivo* displacement of the tracer by unlabeled β-EP, DYN, and EKC (but not by naloxone and DADLE) suggests that the binding sites in the lung have a significant kappa-type property. It was also shown that the lung plays an important role in the distribution of the peptide as a depot after i.v. administration in the rat.

REFERENCES

1. C.H. Li: β-Endorphin. *Cell* 31, 504-505 (1982).

2. J.R. Dave, N. Rubinstein, and R.L. Eskay: Evidence that β-endorphin binds to specific receptors in rat peripheral tissues and stimulates the adenylate cyclase-adenosine 3',5'-monophosphate system. *Endocrinology* **117**, 1389-1396 (1985).

3. K. Kamikubo, H. Murase, M. Murayama, K. Miura, M. Nozaki, and K. Tsurumi: Opioid and non-opioid binding of β-endorphin to bovine adrenal medullary membranes. *Regulatory Peptides* 15, 155-162 (1986).

5. F.M. Leslie, C. Chavkin, and B.M. Cox: Opioid binding properties of brain and peripheral tissues: evidence for heterogeneity in opioid ligand binding sites. *J. Pharmacol. Exp. Ther.* **214**, 395-402 (1980).

6. J. Garzón, R. Schulz, and A. Herz: Evidence for the -type of opioid receptor in the rat vas deferens. *Mol. Pharmacol.* 28, 1-9 (1985).

6. J.C. Sodoyez, F.R. Sodoyez-Goffaux, and Y.M. Moris: ^{125}I-Insulin: kinetics of interaction with its receptors and rate of degradation in vivo. *Am. J. Physiol.* **239**, E3-E11 (1980).

13. M. Berman, E.A., McGuire, J. Roth, A.J., Zeleznik: Kinetic modeling of insulin binding to receptors and degradation in vivo in the rabbit. *Diabetes* 29, 50-59 (1980).

8. J. Philippe, P.A., Halban, A., Gjinovci, W.C. Duckworth, J. Estreicher, and A.E. Renold: Increased clearance and degradation of [^{3}H]insulin in streptozotocin diabetic rats: Role of the insulin-receptor compartment. *J. Clin. Invest.* **67**, 673-680 (1981).

9. K.C. Wilson, R.E. Weitzman, and D.A. Fisher: Arginine vasopressin metabolism in dogs. II. Modeling and system analysis. *Am. J. Physiol.* **235**, E598-E605 (1978).

10. D.C. Whitcomb, T.M. O'Doriso, S. Cataland, M.A. Shetzline, and M.T. Nishikawara: Identification of tissue insulin receptors: Use of a unique in vivo radioreceptor assay. *Am. J. Physiol.* **249**, E561-E567 (1985).

11. H. Sato, Y. Sugiyama, S. Miyauchi, Y. Sawada, T. Iga, and M. Hanano: Pharmacokinetic study of exogenously administered β-endorphin using a rapid radioreceptor assay in rats. *Life Sci.* **35**, 1051-1059 (1984).

12. H. Sato, Y. Sugiyama, Y. Sawada, T. Iga, and M. Hanano: Physiologically based pharmacokinetics of radioiodinated human β-endorphin in rats. An application of the capillary membrane-limited model. *Drug Metab. Dispos.* **15**, 540-550 (1987).

13. H. Sato, Y. Sugiyama, Y. Sawada, T. Iga, and M. Hanano: Binding of radioiodinated human β-endorphin to serum proteins from rats and humans, determined by several methods. *Life Sci.* **1985**, 1309-1318 (1985).

14. J.M. Conlon, J. Whittaker, V. Hammond, and K.G.M. Alberti: Metabolism of somataostatin and its analogues by the liver. *Biochim. Biophys. Acta.* **677**, 234-242 (1981).

15. P. Nicolas, R.G. Hammonds, Jr., S. Gomez, and C.H. Li: β-Endorphin: thermodynamics of the binding reaction with rat brain membranes. *Arc. Biochem. Biophys.* **217**, 80-86 (1982).

16. A. Tsuji, T. Yoshikawa, K. Nishide, H. Minami, M. Kimura, E. Nakashima, T. Terasaki, E. Miyamoto, C.H. Nightingale, and T.

Yamana: Physiologically based pharmacokinetic model for β-lactam antibiotics I: Tissue distribution and elimination in rats. *J. Pharm. Sci.* **72**, 1239-1251 (1983).

17. K. Higaki and M. Fujimoto: Inulin carboxyl-^{14}C and ^{36}Cl spaces of various tissues of the rat. *J. Physiol. Soc. Jpn.* **31**, 164-172 (1969).

18. P. Ferrarra and C.H. Li: β-Endorphin: Radioreceptor binding assay. *Int. J. Peptide Protein Res.* **16**, 66-69 (1980).

19. R.A. Houghten, W.C. Chang, and C.H. Li: Human β-endorphin: synthesis and characterization of analogs iodinated and tritiated at tyrosine residues 1 and 27. *Int. J. Peptide Protein Res.* **16**, 311-320 (1980).

20. G. Lam, M.L. Chen, and W.L. Chiou: Determination of tissue to blood partition coefficients in physiologically-based pharmacokinetic studies. *J. Pharm. Sci.* **71**, 454-456 (1982).

21. H.N. Sapru, R.N. Wilette, and A.J. Krieger: Stimulation of pulmonary J receptors by an enkephalin-analog. *J. Pharmcol. Exp. Ther.* **217**, 228-234 (1981).

Table 1.

Tissue-to-serum concentration ratios (Kp_{app}) of $[^{125}I\text{-}Tyr^{27}]\beta\text{-EP}$ and $^{125}I\text{-}\beta\text{-EP}$ in the Rat

	Kp_{app} of $[^{125}I\text{-}Tyr^{27}]\beta\text{-EP}$[a]		Kp_{app} of $^{125}I\text{-}\beta\text{-EP}$[c]	Fractional IFV[d]
	Tracer only	Tracer + β-EP[b]		
Liver	1.37 ± 0.39	0.35 ± 0.04[e]	0.37 ± 0.03	0.16
Kidney	4.03 ± 0.68	3.50 ± 0.93	2.2 ± 0.22	0.20
Lung	4.46 ± 0.80	1.14 ± 0.29[f]	0.79 ± 0.18	0.19
Muscle	0.21 ± 0.06	0.12 ± 0.01	0.10 ± 0.02	0.12
Adipose	0.14 ± 0.02	0.10 ± 0.02	0.095 ± 0.019	0.14
Gut	0.76 ± 0.18	0.43 ± 0.06	0.23 ± 0.10	0.094
Heart	0.42 ± 0.15	0.17 ± 0.05	0.18 ± 0.01	0.10
Brain	0.068 ±0.027	0.036 ± 0.015	0.038 ± 0.005	0.004
Skin	0.40 ± 0.07	0.38 ± 0.08	0.65 ± 0.17	0.30

a Values are the means ± SE (n = 4).

b Values are the means ± SE (n = 3). Taken from Ref. 12.

c Unlabeled β-EP (48.5 nmole/kg) was simultaneously injected with $[^{125}I\text{-}Tyr^{27}]\beta\text{-EP}$.

d Significantly different ($p<0.05$) from tracer only injection.

e Significantly different ($p<0.02$) from tracer only injection.

f The volume ratio of the interstitial fluid in the tissue, taken from Refs. 15 and 16.

FIGURE LEGENDS

Fig. 1. *Bindings of $[^{125}I\text{-}Tyr^{27}]\beta\text{-EP}$ and $^{125}I\text{-}\beta\text{-EP}$ to rat brain membranes, inhibited by unlabeled human β-EP.*

Each point is the mean of triplicate determination.

Fig. 2. **A.** *The effect of an additional injection of unlabeled β-EP (48.5 nmole/kg) through the femoral vein (●) or carotid artery (○) on the serum concentrations of preadministered $[^{125}I\text{-}Tyr^{27}]\beta\text{-EP}$ in the rat.* **B.** *The effect of an additional injection of unlabeled β-EP (48.5 nmole/kg) through the femoral vein on serum concentrations of preadministered $^{125}I\text{-}\beta\text{-EP}$ in the rat.*

Each point and vertical bar represent the mean ± SEM of three rats in the panels A and B.

Fig. 3. *The effect of an additional injection of 48.5 nmole/kg of DYN (A) or EKC (B), 3.1 μmole/kg of naloxone (C), or 240 nmole/kg of DADLE (D) throught the femoral vein of the serum concentrations of preadministered $[^{125}I\text{-}Tyr^{27}]\beta\text{-EP}$ in the rat.*

Each point and vertical bar represent the mean ± SEM of three rats.

Fig. 1

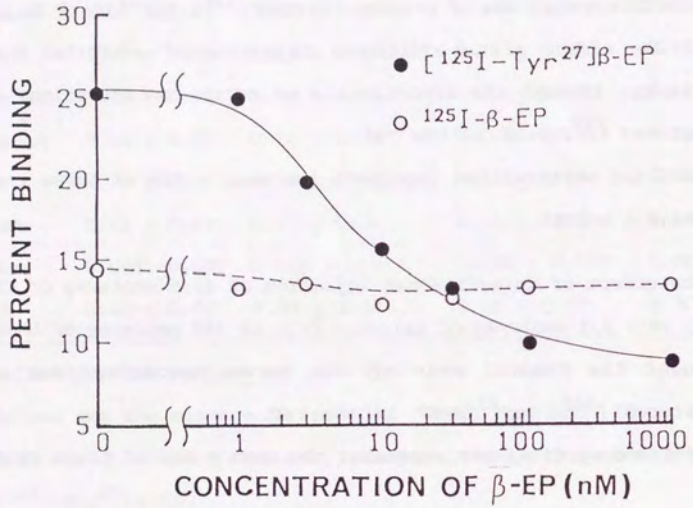
PERCENT BINDING
30
25
20
15
10
5
0
1
10
100
1000
CONCENTRATION OF β-EP (nM)
● [125I-Tyr27]β-EP
○ 125I-β-EP

Fig. 2

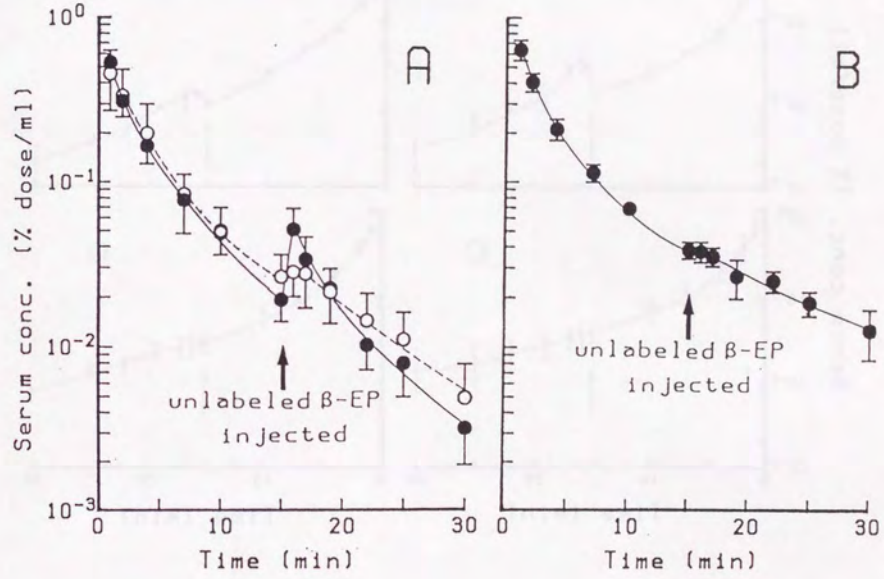
Serum conc. (% dose/ml)
10^0
10^-1
10^-2
10^-3
A
B
unlabeled β-EP
injected
unlabeled β-EP
injected
0
10
20
30
Time (min)
Time (min)

Fig. 3

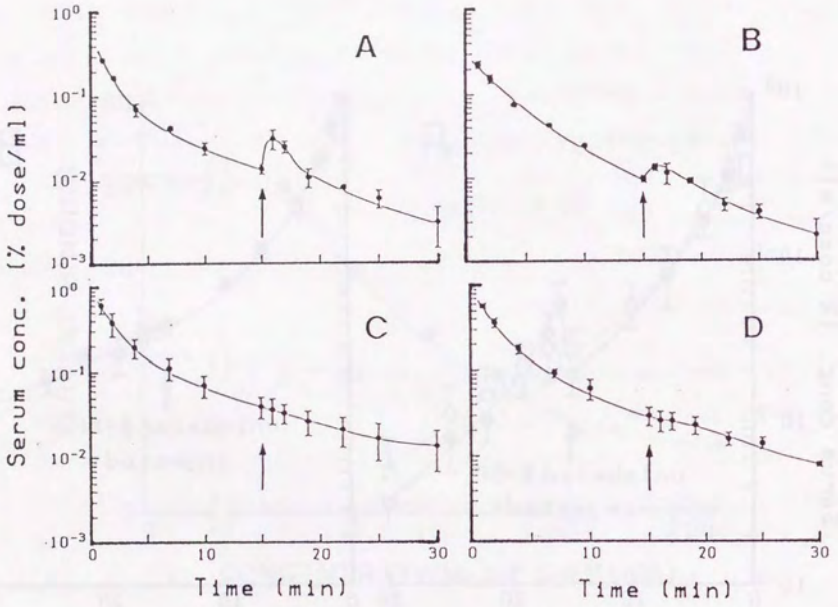
A
B
C
D
Serum conc. (% dose/ml)
10^0
10^{-1}
10^{-2}
10^{-3}
0
10
20
30
Time (min)
Time (min)

PART III

SPECIFIC BINDING AND CLEARANCE OF [^{3}H]DYNORPHIN(1-13) IN THE PERFUSED RAT LUNG: AN APPLICATION OF MULTIPLE-INDICATOR DILUTION METHOD

SUMMARY

The clearance and binding of a kappa-selective opioid peptide, dynorphin(1-13), in the perfused rat lung has been examined, using the multiple indicator dilution method. More than 50% of [^{3}H]dynorphin(1-13) entering the pulmonary circulation was eliminated by the lung during a single passage at a tracer dose. By contrast, when a high dose (100 μM) of dynorphin(1-13) was concomitantly injected, [^{3}H]dynorphin(1-13) behaved like [^{14}C]sucrose, an extracellular marker. The kinetic analyses of the pulmonary venous outflow curves of [^{3}H]dynorphin(1-13) and [^{14}C]sucrose at low and high doses of dynorphin(1-13) indicated that the initial uptake rate constant, extraction ratio and distribution volume of [^{3}H]dynorphin(1-13) decreased significantly in the presence of a high concentration of unlabeled dynorphin(1-13). These lines of evidence suggest that [^{3}H]dynorphin(1-13) is eliminated by a saturable process and binds to a specific binding site in the perfused lung, which may be the kappa-type binding site. The multiple indicator dilution technique, in combination with a moment analysis, was successfully applied to demonstrate the specific binding and clearance of dynorphin(1-13) in the perfused lung.

INTRODUCTION

The lung plays a major role in the regulation of many endogenous substances including polypeptides (1-3) and enkephalins (4-6). The present study describes the contribution of the pulmonary circulation to the clearance of dynorphin(1-13). On the other hand, we have suggested the existence of a kappa-type binding site in the lung (7), which serves as a saturable depot of exogenously administered β-endorphin in vivo. The use of a kappa-selective opioid peptide is adequate to confirm the presence of the putative binding site in the lung. However, in such a complex situation that rapid degradation might occur simultaneously with the binding, a more sophisticated approach should be chosen for this purpose.

In the present study, therefore, the multiple indicator dilution (MID) technique, which has been shown to be a useful tool for measuring the initial uptake rate constant into the liver (8,9), kidney (10,11), and heart (12,13), in combination with a moment analysis (14,15), was applied to verify the putative binding site in the lung using a kappa-selective opioid peptide, dynorphin(1-13) (16), and to evaluate the pulmonary clearance of this peptide. There is little information concerning the pharmacokinetic characteristics of dynorphins except for our transport study of a stable analogue of dynorphin using isolated brain capillaries (17).

MATERIALS AND METHODS

Chemicals. Bovine serum albumin (Fraction V; BSA) was obtained from Sigma Chemical Co. (St. Louis, MO, USA). [^{3}H]Dynorphin(1-13) with a specific activity of 24.4 mCi/μmol, which was labeled at the Amersham International Ltd. (Buckinghamshire, UK), is a gift from Dr. Shinro Tachibana, Eisai Co., Ltd. (Tokyo, Japan). Unlabeled dynorphin(1-13) was obtained from Peptide Institute Inc. (Osaka, Japan), and trichloroacetic acid (TCA) from Wako Pure Chemical Industries., Ltd. (Osaka, Japan). [^{14}C]Sucrose was purchased from New England Nuclear Corp. (Boston, MA). Other chemicals were of analytical grade and used without further purification. [^{3}H]Dynorphin(1-13) dissolved in methanol was stored at -20°C, until it was purified by reverse phase HPLC and lyophilized for use in each experiment.

Lung Perfusion. Adult male Wistar rats (Sankyo Laboratory Co., Ltd., Toyama, Japan), weighing 240-300 g and allowed free access to food and water, were anesthetized with an intraperitoneal injection of sodium pentobarbital (50 mg/kg). The rats were placed on a heating plate (37°C) in a supine position, the trachea cannulated, and ventilated with the humidified room air at a rate of 60 breaths/min and a tidal volume of 2-3 ml using an animal respirator (model KN-56, Natsume Seisakusho Co., Tokyo, Japan). The lung was operated by a method previously described (18). Briefly, the chest was opened, the animals were intravenously injected with heparin (1,000 U/kg), the main pulmonary artery and left ventricle (into the pulmonary vein via mitral valve) were cannulated, and the single-pass perfusion was started immediately after exsanguination by cutting the aorta. The perfusate was composed of 4.5% (wt/vol) BSA, 10 mM glucose in Krebs-Ringer bicarbonate (KRB) buffer (NaCl, 119 mM; KCl, 4.73 mM; $CaCl_2 2H_2O$, 2.54 mM; KH_2PO_4, 1.18 mM; $MgSO_4\ 7H_2O$, 1.18 mM; $NaHCO_3$, 24.9 mM; pH = 7.4), oxygenated with 95% O_2-5% CO_2, and contained in a reservoir in a thermostatic water bath. The lung was maintained at 37°C and perfused at an effective perfusion pressure of 15 cm H_2O at the inlet of the organ and a constant flow rate of 8.6 mL·min^{-1} using a peristaltic pump (model MP, Tokyo Rikakikai Co, Tokyo, Japan). In order to assess the degradation of [^{3}H]dynorphin(1-13) in the reservoir perfusate, a TCA-precipitation method was used as described later.

MID Method. The pulmonary uptake rate of [^{3}H]dynorphin(1-13) was measured by the MID method as previously described for the liver (Goresky & Bach 1970). After a 15-min stabilization period, the 100 μl of perfusate containing [^{3}H]dynorphin(1-13) (0.2 μCi/ml) and [^{14}C]sucrose (0.04 μCi/ml), as an extracellular reference marker, was rapidly injected with or without 100 μM dynorphin(1-13) into the pulmonary artery. The venous outflow was collected from the pulmonary vein cannula in serial tubes at the rate of one tube per second for 30 sec. Two aliquots from each tube were obtained: one (50 μl) for the determination of the total [^{3}H]- ([^{3}H-T]) and [^{14}C]-radioactivity, and the other (50 μl) for determination of unchanged [^{3}H]dynorphin(1-13) by TCA precipitation (see Analytical Method), using the double-isotope counting method with an appropriate crossover correction in a liquid scintillation counter (model LSC-700, Aloka Co., Tokyo, Japan). In each perfused lung preparation, two bolus injections were performed using the solutions with and without 100 μM unlabeled dynorphin(1-13), and the second dilution curve was obtained 2 min after the first curve. In each perfusion experiment, the tracer amount of

[^{3}H]dynorphin(1-13) was given first and then the coinjection of labeled and unlabeled dynorphin(1-13) was performed, in order to avoid a possible effect of unlableled peptide remaining in the lung on the subsequent injection of labeled peptide alone.

Analytical Method. For estimating intact [^{3}H]dynorphin(1-13) in the outflow perfusate, a TCA precipitation method was employed according to the method described previously (19). Perfusate samples (50 µl) were mixed well with an equal volume of 40% (wt/vol) TCA solution and 20 µl of rat serum as a precipitation carrier. These mixtures were kept standing at 4°C for 30 min, centrifuged at 3,000 x *g* for 15 min, and the supernatants were transferred into separate tubes by aspiration. The [^{3}H]-radioactivity in the supernatants ([^{3}H-S]) was measured in a liquid scintillation counter (model ARC-605, Aloka Co.). The [^{3}H]-radioactivity in the precipitate was calculated as [^{3}H-T] minus [^{3}H-S], and taken as intact [^{3}H]dynorphin(1-13).

Data Analysis. The radioactivity in each sample was normalized by dividing it by the injected dose, so that the outflow patterns of [^{3}H]dynorphin(1-13) and [^{14}C]sucrose could be adequately compared. The concentrations in the effluent were thus expressed as the outflow fractions of the dose per ml. During a short time interval when any efflux can be considered to be negligible, the appearance rate constant for pulmonary uptake of dynorphin(1-13) was obtained from MID experiments, using the following equation (8):

$$\ln[FC(t)_{suc}/FC(t)_{dyn}] = k_1\lambda t/(1 + \gamma) = k_{1,app}\cdot t \quad (1)$$

where $FC(t)_{suc}$ and $FC(t)_{dyn}$ denote the fractional concentrations of [^{14}C]sucrose and [^{3}H]dynorphin(1-13) per ml of perfusate effluent at time t, respectively; k_1 is the net rate constant for the uptake; λ is

the ratio of the cellular space to the vascular space; and γ is the ratio of the interstitial space to the vascular space. Thus, $\lambda/(1 + \gamma)$ represents the ratio of cellular space to extracellular space. According to Eq. (1), the plot of the logarithm of the ratio of the outflow fraction of the test compound to that of an extracellular reference should yield a straight line, and the apparent rate constant for the influx process, $k_{1,app}$, was determined from the slope of this line by a least-squares regression analysis.

Since the injected radioactivity of [^{14}C]sucrose was almost completely recovered in the effluent, the pulmonary extraction (E) of [^{3}H]dynorphin(1-13) was obtained in relation to the recovery ratio of [^{14}C]sucrose as:

$$E = 1 - \Sigma FC(t)_{dyn}/\Sigma FC(t)_{suc} \quad (2)$$

Moreover, the mean transit time ($\bar{t}$) and the apparent distribution volume (Vd) of each labeled compound were calculated according to a model-independent moment analysis (14,15) as follows:

$$\bar{t} = \Sigma t\cdot FC(t)/\Sigma FC(t) \quad (3)$$

$$Vd = Q\cdot\bar{t}/(1 - E) \quad (4)$$

where Q denotes the perfusion flow rate. The significance of differences between the MID experiments in the absence and presence of 100 µM dynorphin(1-13) was assessed by means of paired Student's *t*-test.

RESULTS AND DISCUSSION

The present study was designed to verify the kappa-type binding site in the lung, which has been suggested to play an important role in the distribution of intravenously administered β-endorphin (7), using the multiple indicator dilution method. For this purpose, a kappa-selective opioid peptide, dynorphin(1-13), was used as a tracer ligand.

The lung has been recognized as having an important role in regulating the systemic concentration of a variety of vasoactive amines, prostaglandins and polypeptides (1-3) by selective removal or metabolism. Moreover, the anatomical location renders a unique significance to the lung, because it is in direct equilibrium with the arterial blood, and intravenously injected substances are subject to first-pass metabolism through the lung before they reach the systemic circulation. Considering that significant metabolism of enkephalins occurs in the pulmonary circulation (4-6), it seems important to quantitatively evaluate the pulmonary clearance of dynorphin(1-13) for its in vivo efficacy.

During the lung perfusion experiment, there was no appearance of edema, where the perfusion flow rates were constant at 8.55 $\pm$ 0.25 mL·min^{-1} (mean $\pm$ s.e.m.; n = 5), and the variation in perfusion pressure was less than $\pm$5%. Figures 1A and 1B show typical sets of pulmonary venous outflow curves for [^{3}H]dynorphin(1-13) and [^{14}C]sucrose in the perfused rat lung in the absence (tracer dose) and presence of 100 μM unlabeled dynorphin(1-13) (high dose) in the injection solution, respectively. After an initial delay (catheter transit time), both materials appeared in the outflow, reached peak concentration in several seconds, and then declined exponentially with time. It is

obvious that the outflow patterns of these labeled compounds were similar at the high dose of dynorphin(1-13), while that of [^{3}H]dynorphin(1-13) was much lower than that of [^{14}C]sucrose, indicating a saturable clearance of [^{3}H]dynorphin(1-13) by the lung. There was no significant difference in the outflow pattern of [^{14}C]sucrose between low and high doses of dynorphin(1-13). The ratio plots of $\ln(FC_{suc}/FC_{dyn})$ vs. time at the low and high doses of dynorphin(1-13) are shown in Fig. 2. The initial slope of the ratio plot ($k_{1,app}$) of [^{3}H]dynorphin(1-13) at a high dose was significantly lower than that at a low dose, indicating that the uptake of dynorphin(1-13) is a saturable process.

The concentration of [^{3}H]dynorphin(1-13) in the injectate was 8.2 nM, as calculated from its relatively low specific activity. However, from the injection volume (100 μl) and the calculated Vd of [^{3}H]dynorphin(1-13) (2.08 mL), the average concentration of the tritiated peptide in the lung is estimated to be less than 0.4 nM. Thus, the use of a low concentration of [^{3}H]dynorphin(1-13) could make it possible to investigate the putative kappa-type binding site in the lung. The kinetic parameters for [^{3}H]dynorphin(1-13) and [^{14}C]sucrose in the perfused lungs were calculated using Eqs.(1)-(4), and are listed in Table 1. The catheter transit time ($\bar{t}_{cat}$) was 1.51 $\pm$ 0.02 sec (mean $\pm$ s.e.m.; n = 5), as calculated from the catheter volume (V_{cat}) of 0.143 mL and the perfusion flow rate in each perfusion experiment. The obtained mean transit times and distribution volumes of [^{3}H]dynorphin(1-13) and [^{14}C]sucrose (Table 1) reflect the behaviors of these materials in the lung, because $\bar{t}_{cat}$ (1.5 sec) and V_{cat} (0.14 mL) are small relative to the corresponding values of t and

Vd. The Vd value of [^{14}C]sucrose (approximately 1 mL) could be appropriately assigned to the sum of the catheter volume (0.143 mL) and the extracellular fluid volume of the rat lung, i.e., the capillary bed volume (0.55 mL) and interstitial fluid volume (0.3 mL) reported previously (20).

Since the pulmonary extraction ratio of [^{3}H]dynorphin(1-13) was determined as high as 0.57 (Table 1), the lung appears to be an important disposing organ for rapidly clearing dynorphin(1-13) from the circulation. As inspected from Table 1, the extraction of [^{3}H]dynorphin(1-13) was significantly inhibited by a high dose of dynorphin(1-13). Moreover, the percentage of intact [^{3}H]dynorphin(1-13) in the effluent also significantly increased in the presence of unlabeled dynorphin(1-13) (results not shown). These results indicate that the effective pulmonary clearance of [^{3}H]dynorphin(1-13) is a saturable process, which may be explained by the peptidase enzymes of the pulmonary endothelium (21,22). However, it is unlikely that the association of [^{3}H]dynorphin(1-13) with hydrolytic enzymes located on the surface of the pulmonary endothelium would take several seconds (Fig. 2). An alternative explanation is that the polypeptides cannot permeate through the cellular membranes because of their low hydrophobicity and relatively large molecular size, and the observed initial uptake rate is due to the association process of dynorphin(1-13) to a certain binding site, as comprehensively described for the hepatic uptake of epidermal growth factor (23).

The mean transit times ($\bar{t}$) of [^{3}H]dynorphin(1-13) and [^{14}C]sucrose were not significantly different with each other, and no significant change of t was observed between the absence and presence of unlabeled dynorphin(1-13) in the injection solution (Table 1). This observation

apparently indicates that interactions of [^{3}H]dynorphin(1-13) with the plasma membranes of lung alveolar cells and/or the surface of pulmonary endothelium did not significantly alter the transit time of this peptide. However, the diffusibity of dynorphin(1-13) and sucrose within the extracellular cell matrix could be different, and the transit time is not so sensitive to an early association process as to an efflux process, due to its nature as a second-order moment parameter. Consequently, the above observation does not necessarily mean that dynorphin(1-13) lacks any interactions with certain components of the lung tissue.

Table 1 also indicates that the Vd of [^{3}H]dynorphin(1-13) at the high dose (100 μM) is not significantly different from that of [^{14}C]sucrose, suggesting that this peptide behaves like sucrose, an extracellular marker, when its specific binding is effectively blocked. This observation also suggests that the capillary permeability of dynorphin(1-13) is similar to that of sucrose and is not the limiting step for its distribution into the lung. On the other hand, the Vd of [^{3}H]dynorphin(1-13) in the absence of unlabeled dynorphin(1-13) is significantly greater than that in the presence, suggesting a saturable distribution of dynorphin(1-13) into the lung. The 38% decrease of Vd in the presence of excess dynorphin(1-13), together with the above mentioned 54% decrease of $k_{1,app}$, suggests the existence of a specific binding site for dynorphin(1-13) in the lung, in support of the previous in vivo evidence for the pulmonary kappa-type binding capacity (7). The results presented in this study might well be explained by a receptor-mediated degradation in which the ligand binding is coupled to subsequent peptidase degradation, as

previously suggested for the enkephalin degradation in the brain (24). However, more detailed study should be required to examine the relationship between the enzymatic degradation and the specific binding of dynorphin(1-13) in the lung.

In conclusion, the multiple-indicator dilution method was successfully applied to demonstrate the specific binding and clearance of kappa-selective opioid peptide, dynorphin(1-13), in the perfused rat lung.

Acknowledgments

The authors wish to thank Dr. Shinro Tachibana, Tsukuba Research Laboratory of Eisai Co., Ltd., for the generous gift of [^{3}H]dynorphin(1-13), and are grateful to Mr. Kazuyoshi Takeda and Ms. Mitsue Yamaguchi for their technical assistance. This study was supported by a Grant-in-Aid for Scientific Research from the Ministry of Education, Science and Culture of Japan, and Project Research Fund from the Graduate School of Natural Science and Technology, Kanazawa University.

REFERENCES

1. Y.S. Bakhle and J.R. Vane: Pharmacokinetic function of the pulmonary circulation. *Pharmacol. Rev.* **54**, 1007-1045 (1974).
2. J.W. Ryan: Processing of endogenous polypeptides by the lungs. *Ann. Rev. Physiol.* **44**, 241-255 (1982).
3. J.R. Bend, C.J. Serabjit-Singh, and R.M. Philpot: The pulmonary uptake, accumulation, and metabolism of xenobiotics. *Ann. Rev. Pharmacol. Toxicol.* **25**, 97-125 (1985).
4. D. Manwaring and K. Mullane: Disppearance of enkephalins in the isolated perfused rat lung. *Life Sci.* **35**, 1787-1794 (1984).
5. P.A. Crooks, J.W. Krechniak, J.W. Olson, and M.N. Gillespie: High-performance liquid chromatographic analysis of pulmonary metabolites of leu- and met-enkephalins in isolated perfused rat lung. *J. Pharm. Sci.* **74**, 1010-1020 (1985).
6. M.N. Gillespie, J.W. Krechniak, P.A. Crooks, R.J. Altiere, and J.W. Olson: Pulmonary metabolism of exogenous enkephalins in isolated perfused rat lungs. *J. Pharmacol. Exp. Ther.* **232**, 675-681 (1985).
7. H. Sato, Y. Sugiyama, Y. Sawada, T. Iga, and M. Hanano: In vivo evidence for the specific binding of human β-endorphin to the lung and liver of the rat. *Biochem. Pharmacol.* **37**, 2273-2278 (1988).
8. C.A. Goresky and G.G. Bach: Membrane transport and the hepatic circulation. *Ann. N.Y. Acad. Sci.* **170**, 18-45 (1970).
9. S.C. Tsao, Y. Sugiyama, Y. Sawada, S. Nagase, T. Iga, and M. Hanano: J. Pharm. Sci. 72: 1239-1251. *J. Pharmacokin. Biopharm.* **14**, 51-64 (1986).
10. Effect of albumin on hepatic uptake of warfarin in normal and

analbuminemic mutant rats: analysis by multiple indicator dilution method, M. Silverman, M.A. Aganon, and F.P. Chinard: D-Glucose interactions with renal tubular cell surfaces. *Am. J. Physiol.* **218**, 735-742 (1970).

11. N. Itoh, Y. Sawada, Y. Sugiyama, T. Iga, and M. Hanano: Kinetic analysis of rat renal tubular transport based on multiple-indicator dilution method. *Am. J. Physiol.* **251**, F103-F114 (1986).
12. W.H. Ziegler and C.A. Goresky: Kinetics of rubidium uptake in the working dog heart. *Cir. Res.* **29**, 208-220 (1971).
13. J. Kuikka, M. Levin, and J.B. Bassingthwaighte: Multiple tracer dilution estimates of D- and 2-deoxy-D-glucose uptake by the heart. *Am. J. Physiol.* **250**, H29-H42 (1986).
14. K. Yamaoka, T. Nakagawa, and T. Uno: Statistical moments in pharmacokinetics. *J. Pharmacokin. Biopharm.* **6**, 547-558 (1978).
15. T. Kakutani, K. Yamaoka, M. Hashida, and H. Sezaki: A new method for assessment of drug disposition in muscle: application of statistical moment theory to local perfusion systems. *J. Pharmacokin. Biopharm.* 13, 609-631 (1985).
16. C. Chavkin, I.F. James, and A. Goldstein: Dynorphin is a specific endogenous ligand of the -opioid receptor. *Science* **215**, 413-415 (1982).
17. T. Terasaki, K. Hirai, H. Sato, Y.S. Kang, and A. Tsuji: Absorptive-mediated endocytosis of a dynorphin-like analgesic peptide, E-2078, into the blood-brain barrier. *J. Pharmacol. Exp. Ther.* **251**, 351-357 (1989).
18. B.R. Smith and J.R. Bend: Lung perfusion techniques for xenobiotic

metabolism and toxicity studies. *Methods in Enzymology* **77**, 105-120 (1981).

19. H. Sato, Y. Sugiyama, Y. Sawada, T. Iga, and M. Hanano: Physiologically based pharmacokinetics of radioiodinated human β-endorphin in rats: an application of the capillary membrane-limited model. *Drug Metab. Dispos.* **15**, 540-550 (1987).
20. A. Tsuji, T. Yoshikawa, K. Nishide, H. Minami, M. Kimura, E. Nakashima, T. Terasaki, E. Miyamoto, C.H. Nightingale, and T. Yamana: Physiologically based pharmacokinetic model for β-lactam antibiotics I: tissue distribution and elimination in rats. *J. Pharm. Sci.* **72**, 1239-1251 (1983).
21. J.W. Ryan: Metabolic activity of pulmonary endothelium: modulations of structure and function. *Ann. Rev. Physiol.* **48**, 263-277 (1986).
22. J.W. Ryan: Peptidase enzymes of the pulmonary vascular surface. *Am. J. Physiol.* **257**, L53-L60 (1989).
23. H. Satoh, Y. Sugiyama, Y. Sawada, S. Sakamoto, T. Fuwa, and M. Hanano: Dynamic determination of kinetic parameters for the interaction between polypeptide hormones and cell-surface receptors in the perfused rat liver by the multiple-indicator dilution method. *Proc. Natl. Acad. Sci. USA.* **85**, 8355-8359 (1988).
24. M. Knight and W.A. Klee: The relationship between enkephalin degradation and opiate receptor occupancy. *J. Biol. Chem.* 253, 3843-3847 (1978).

Table 1.

Apparent initial uptake rate constant, extraction ratio, mean transit time and distribution volume of [^{3}H]dynorphin(1-13) and [^{14}C]sucrose at low and high doses of unlabeled dynorphin(1-13) in the perfused rat lungs.

Parameter[a]	[^{3}H]Dynorphin(1-13)		[^{14}C]Sucrose	
	Low dose[b]	High dose[c]	Low dose[b]	High dose[c]
$k_{1,app}$ (sec^{-1})	0.12 ± 0.017	0.055 ± 0.013*	-	-
E	0.568 ± 0.042	0.228 ± 0.110*	0	0
$\bar{t}$ (sec)	5.84 ± 1.09	6.31 ± 1.22	7.43 ± 0.71	7.75 ± 0.76
Vd (mL)	2.08 ± 0.48	1.29 ± 0.29*	1.06 ± 0.10	1.10 ± 0.91

The values are expressed as means ± s.e.m. (n = 5).

[a] The kinetic parameters were calculated by Eqs. (1)-(4).

[b] The concentration of [^{3}H]dynorphin(1-13) in the injectate was 8.2 nM.

[c] The concentration of dynorphin(1-13) in the injectate was 100 μM.

* $P < 0.05$, significantly different from the low dose injection of dynorphin (1-13).

FIGURE LEGENDS

Fig. 1. *Typical sets of pulmonary venous outflow curves for [^{3}H]dynorphin (●) and [^{14}C]sucrose (○) in the perfused rat lung in the absence (panel A) and presence (panel B) of 100 μM unlabeled dynorphin(1-13) in the injection solution.*

Fig. 2. *The ratio of [^{14}C]sucrose to [^{3}H]dynorphin(1-13) fractional concentrations per milliliter plotted against time at the low (●) and high (○) doses of dynorphin(1-13) in the perfused rat lungs.*

Each point and vertical bar represent the mean ± SEM from five rats.

Fig. 1

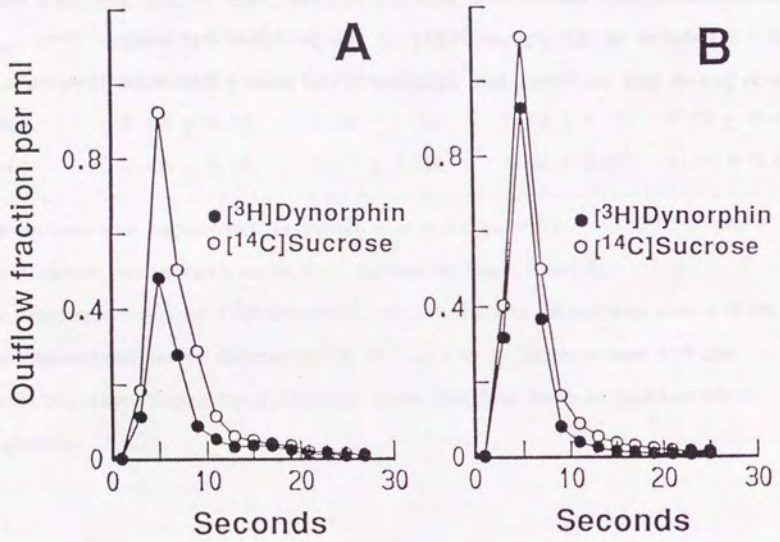
A
B
Outflow fraction per ml
0.8
0.4
0
●[3H]Dynorphin
○[14C]Sucrose
0
10
20
30
Seconds

Fig. 2

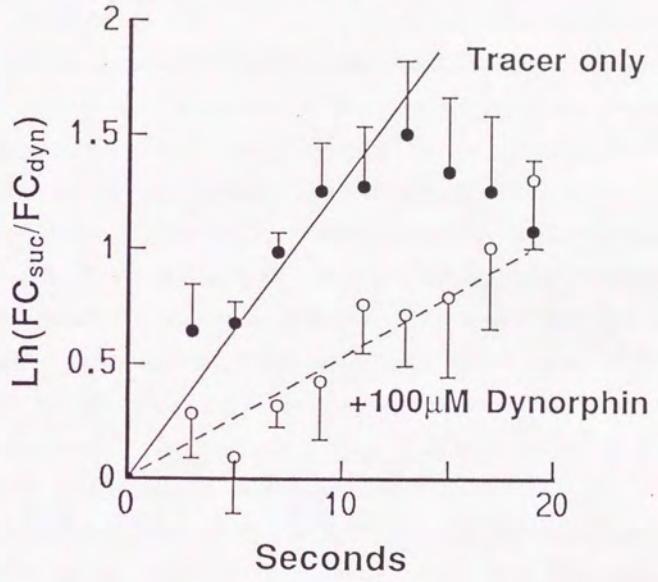
Ln(FCsuc/FCdyn)
2
1.5
1
0.5
0
Tracer only
+100μM Dynorphin
0
10
20
Seconds

PART IV

SPECIFIC BINDING OF β-ENDORPHIN TO THE ISOLATED RENAL BASOLATERAL MEMBRANES IN VITRO

SUMMARY

Binding of human β-endorphin (β-EP) to rat renal basolateral membranes was characterized using [^{125}I]Tyr^{27}-β-EP ([^{125}I]β-EP) as a primary ligand. Ten milimolar of EDTA completely inhibited the degradation of [^{125}I]β-EP in the incubation mixture at 4°C, thus making it possible to examine the [^{125}I]β-EP binding in a quantitative manner. The specific binding of [^{125}I]β-EP to the basolateral membranes was reversible and saturable, and a nonlinear least-squares regression analysis of a saturation isotherm revealed two different classes of specific binding sites. One class had an apparent dissociation constants (Kd) of 0.68 nM and a lower number of binding sites (33 fmol/mg protein), whereas the other class had a lower affinity (apparent Kd of 210 nM) and a higher number of binding sites (7.3 pmol/mg protein). Inhibition of the [^{125}I]β-EP binding by naloxone (10 μM) was approximately only 20% and that by D-Ala^2-D-Leu^5-enkephalin (10 μM) was null, suggesting the major role of a non-opioid binding component in the specific [^{125}I]β-EP binding to the basolateral membranes. Moreover, 50% inhibition by 10 μM of dynorphin(1-13) suggests that some region of the primary structure of β-EP, excluding at least the NH_2-terminal enkephalin sequence, is of particular importance for the [^{125}I]β-EP binding. These lines of evidence suggest the exsitence of two different classes of specific binding sites for β-EP on the renal basolateral membranes, and the high- and low-affinity bindings may be attributed to opioid and non-opioid receptors, respectively, as judged by known characteristics opioid and non-opioid receptors in other peripheral tissues.

INTRODUCTION

β-Endorphin (β-EP) is a 31-residue endogenous peptide with potent opioid properties.[1] Since the specific binding sites of β-EP have been found not only in the brain but also in several peripheral tissues,[2-6] increasing attention has been paid to the peripheral direct endorphin actions. Recent studies have revealed that peripheral specific binding and actions of β-EP have been characterized as non-opioid in nature.[3,4,7-10] Dave *et al.*[4] have suggested the existence of two different classes of binding sites of ^{125}I-labeled acetyl-human β-EP on crude membranes prepared from homogenates of several peripheral tissues such as kidney.

In the kidney, specific receptors for various polypeptide hormones have been identified on the basolateral membranes[11-14] and their physiological roles have been implicated in relation to the hormone levels in the systemic circulation.[15,16] However, whether there is specific binding sites of β-EP on the basolateral side of renal tubule cells remains to be known at present, although β-EP was reported as a kidney trophic hormone.[17] Our recent study[2] using *in vivo* labeling technique demonstrated the specific binding of intravenously administered [^{125}I]β-EP to the lung and liver of the rat under the physiological condition, but failed to significantly show specific [^{125}I]β-EP binding to the kidney, possibly due to a high degree of nonspecific binding and/or reabsorption of the peptide *via* the filtration-luminal uptake route.[18] Therefore, in this study, we examined whether specific binding sites of β-EP exist on the isolated basolateral membranes by *in vitro* binding experiments.

MATERIALS AND METHODS

Chemicals. (3-[^{125}I]Iodotyrosyl^{27})human-β-endorphin (~ 2,000 Ci/mmol, designated as [^{125}I]β-EP) and (3-[^{125}I]iodotyrosyl^{A14})human-insulin (~2,000 Ci/mmol, designated as [^{125}I]insulin) were purchased from Amersham International Ltd. (Buckinghamshire, UK) and trichloroacetic acid (TCA), N-ethylmaleimide (NEM) and ethylenediaminetetraacetic acid (EDTA) dipotassium salt from Wako Pure Chemical Industries, Ltd. (Osaka, Japan). Unlabeled β-EP, naloxone, D-Ala^2-D-Leu^5-enkephalin (DADLE), bovine serum albumin (BSA, fraction V), bestatin and bacitracin were obtained from Sigma Chemical Co. (St. Louis, MO), dynorphin(1-13) from Peptide Institute Inc. (Osaka, Japan), and polyethyleneimine (MW, 60,000-80,000) from Nakarai Chemicals, Ltd. (Kyoto, Japan). All other reagents were commercially available and of analytical grade. The peptidase inhibitors (EDTA, bestatin, bacitracin and NEM) and unlabeled opioid ligands (β-EP, naloxone, dynorphin(1-13) and DADLE) were dissolved in 25 mM Tris-HCl buffer (pH 7.4) containing 0.1% BSA. The monoiodinated β-EP was dissolved in phosphate buffered saline (PBS) containing 0.1% BSA and stored at -20°C until study. The labeled β-EP used was at least 98% pure as assayed by a TCA-precipitation method.[19] Distilled, deionized water was used throughout the experiments.

Preparation of Basolateral Membranes. Basolateral membranes were isolated from the renal cortex from male Wistar rats (200-300g, Sankyo Laboratory Co., Toyama, Japan) by the method of Percoll density gradient centrifugation.[20] The obtained membranes were finally suspended in 25 mM Tris-HCl buffer (pH 7.4) containing 300 mM mannitol, and stored in a small volume at -70°C until use.

The purity of the basolateral membranes was assessed by the

determinations of the activities of marker enzymes. Moreover, in order to confirm whether hormone receptors remain active on the basolateral membrane preparations obtained, the specific binding of [^{125}I]insulin in the basolateral membrane suspension was examined in the presence of a peptidase inhibitor, NEM (1 mM), as previously described.[11)]

β-Endorphin Binding Assays. For the binding assays of [^{125}I]β-EP, basolateral membrane fractions were thawed and diluted in 25 mM Tris-HCl buffer (pH 7.4) containing 300 mM mannitol to give a protein concentration of approximately 5 mg/ml. Forty microliters of the membrane suspension was mixed with 80 µl of 25 mM Tris-HCl buffer (pH 7.4) containing 0.125% BSA and 12.5 mM EDTA (designated as incubation buffer; EDTA was not included in case the degradatation of [^{125}I]β-EP was assessed) with and without an unlabeled opioid ligand. Then 80 µl of [^{125}I]β-EP (0.04 µCi, 0.1 nM in a final concentration) dissolved in the incubation buffer was added, and allowed to incubate at 4°C or 25°C in a final volume of 200 µl for 90 min (except when equilibration time of [^{125}I]β-EP binding was examined). The incubation was terminated by filterating the assay mixture under low vacuum through Whatman GF/C filters presoaked with ice-cold 50 mM Tris-HCl buffer (pH 7.4) containing 0.1% BSA and 0.1% polyethyleneimine (designated as presoaking buffer). The filters were then washed twice with additional 5 ml of ice-cold 25 mM Tris-HCl buffer (pH 7.4) containing 0.1% BSA. The ^{125}I-radioactivity on the filters was determined in a γ-counter (model ARC-605, Aloka Co., Tokyo, Japan).

In order to assess the degradation of [^{125}I]β-EP during the binding assay experiments, incubation was performed at 4°C or 25°C in the presence and absence of peptidase inhibitors (i.e., EDTA, bestatin,

bacitracin and NEM). At designated times, the incubation mixitures (200 µl) were added into 200 µl of 15% TCA aqueous solution containing 1% BSA (as a precipitation carrier), mixed well, and the total radioactivity was counted in a γ-counter. Then the mixtures were rapidly filtered under low vacuum through a GF/C filter, and the radioactivity on the filters was measured as TCA-insoluble radioactivity. Thus, the percentage of unchanged [^{125}I]β-EP in the incubation midium was estimated from TCA-insolubility calculated as follows:

$$\text{TCA-insolubility (\%)} = (\text{TCA insoluble cpm})/(\text{total cpm}) \times 100 \quad (1)$$

To demonstrate reversibility of the [^{125}I]β-EP binding, basolateral membranes were incubated with 0.1 nM [^{125}I]β-EP at 4°C for 30 min; thereafter a high concentration (10 µM final) of unlabeled β-EP was added to the incubation mixture and total binding was determined at serial time intervals after β-EP addition.

In saturation experiments, nonspecific binding of [^{125}I]β-EP was defined as the amount (fmol per mg protein) bound to basolateral membranes which was not inhibited by 10 µM of unlabeled β-EP. Specific binding was, therefore, defined as the amount of total binding minus nonspecific binding.

Analytical Methods. Enzyme activities for Na^+,K^+-ATPase, alkaline phosphatase, γ-glutamyltransferase, acid phosphatase, succinate dehydrogenase and lactate dehydrogenase were measured by the methods of Scharschmidt *et al.*,[21)] Walter and Schutt,[22)] Orlowski and Meister,[23)] Rothstein and Blum,[24)] King[25)] and Scalera *et al.*,[26)] respectively. Protein concentration was determined by the method of Bradford,[27)] using the Bio-Rad protein assay kit (Bio-Rad, Richmond, CA) with BSA as a standard.

Data Analysis. Data from saturation experiments were analyzed using the following equation:

$$C_b/P = Bmax_1 \cdot C_f/(Kd_1 + C_f) + Bmax_2 \cdot C_f/(Kd_2 + C_f) \quad (2)$$

where P represents the protein concentration (mg/ml); C_b and C_f are the specifically bound and unbound concentrations (nM) of β-EP in the assay mixtures, respectively; $Bmax_1$ and $Bmax_2$ are the binding capacity (pmol/mg protein) on basolateral membranes at sites 1 and 2, respectively; and Kd_1 and Kd_2 are the affinity constants (nM) at sites 1 and 2, respectively. The left-side hand represents the amount of bound β-EP (pmol) per mg protein of the incubation mixture, which was measured in the above-mentioned binding experiments. Thus, C_f vs. C_b/P curve was fitted to Eq. 2 to estimate the values of $Bmax_1$, Kd_1, $Bmax_2$ and Kd_2, using an iterative nonlinear least-squares regression curve-fitting program, MULTI.[28] Moreover, data from the saturation experiments were expressed as the Scatchard plots using the following linear equation:

$$C_b/P/C_f = -(C_b/P - Bmax_i)/Kd_i \quad (3)$$

where $Bmax_i$ and Kd_i denote the binding kinetic parameters for the i-th binding site.

RESULTS AND DISCUSSION

The previous *in vitro* studies have identified opioid receptors in the kidney[4,29,30] but have not yet provided an evidence for the presence of opioid receptors on the basolateral membranes. Therefore, the present study was designed to demonstrate the specific binding of β-EP to the basolateral membranes prepared from rat renal cortex. The degree of purification of basolateral membranes was determined by measurement of the specific activities of the several marker enzymes: Na^+,K^+-ATPase, the marker enzyme for basolateral membranes, was enriched 19.3 ± 0.7 folds (mean ± SEM; n = 12) with respect to the initial homogenate. On the other hand, alkaline phosphatase and γ-glutamyltransferase, the marker enzymes for the brush-border membranes, were enriched only 1.82 ± 0.16 (mean ± SEM; n = 12) and 1.59 ± 0.12 folds (n = 4), respectively. Contaminations of acid phosphatase derived from lysosomes, succinate dehydrogenase from mitochondria and lactate dehydrogenase from cytoplasm were small, as judged by their enrichment factors of 2.22 ± 0.16, 0.318 ± 0.074 and 0.067 ± 0.005 (mean ± SEM; n = 3), respectively. These enrichment factors of marker enzymes indicate that the isolated membrane fraction was properly purified and sufficiently rich in the basolateral membrane. Moreover, the isolated basolateral membrane fraction exhibited a significant specific binding activity for [^{125}I]insulin (result not shown), the presence of insulin receptors on the membranes was confirmed. Therefore, the obtained membrane fraction was considered to be adequate for the investigation of opioid receptors at the basolateral side of renal tubule cells *in vitro*.

In preliminary experiments of β-EP binding assays, we attempted to minimize the adsorption of [^{125}I]β-EP to GF/C filters without

basolateral membranes in assay tubes. In the absence of BSA and polyethyleneimine in the presoaking buffer, the percentage of adsorped [^{125}I]β-EP to the filteres was as high as 71.1 ± 1.3% (mean ± SEM; n = 3) of the total amount of β-EP applied. By contrast, when 0.1% BSA and 0.1% polyethyleneimine were added to the presoaking buffer, the percentages of adsorped [^{125}I]β-EP were only 1.6 ± 0.3% and 7.2 ± 2.8% (mean ± SEM; n = 3), respectively. Therefore, both 0.1% BSA and 0.1% polyethyleneimine were routinely included in the presoaking buffer thereafter.

In degradation experiments, we determined the optimal conditions required to preserve the stability of [^{125}I]β-EP during the incubation necessary for binding studies. Figure 1 presents the degradation of [^{125}I]β-EP in the incubation mixtures under different conditions. Upon exposure to renal basolateral membranes (1 mg protein/ml) at 4°C, [^{125}I]β-EP was rapidly degraded in the absence of peptidase inhibitors. However, in the presence of either EDTA (10 mM) or other peptidase inhibitors (bestatin 0.1 mM, bacitracin 50 μM and NEM 1 mM), the degradation was markedly reduced. Especially, 10 mM EDTA could completely inhibit the degradation of [^{125}I]β-EP at 4°C, whereas its inhibitory effect was somewhat diminished at 25°C (Fig. 1). Therefore, we routinely added 10 mM EDTA in the assay mixture to avoid the degradation of [^{125}I]β-EP during the binding assays at 4°C. These results suggest that metallopeptidases are involved, at least in part, in the [^{125}I]β-EP degradation in the basolateral membrane suspensions. In the brain, the inactivation of the enkephalins has been suggested to proceed *via* the action of two membrane-bound peptidases;[31a,b] one of these is an aminopeptidase characterized by its sensitivity to

inhibition by bestatin. The second peptidase, originally given the name "enkephalinase", has been shown to be a neutral metallopeptidase with a specificity directed toward cleavage on the amino side of hydrophobic amino acids. The latter enzyme has been shown to be abundantly distributed in the kidney and lung, which is consistent with the present results of rapid [^{125}I]β-EP degradation at neutral pH at 4°C.

As illustrated in Fig. 2, the amount of [^{125}I]β-EP that binds to basolateral membranes varied as a function of the protein concentration. With a protein concentration between 0.2 and 1.5 mg/ml, a linear increase in total and nonspecific binding of [^{125}I]β-EP (0.1 nM) was noted ($r = 0.99$). Therefore, the protein concentration of 1.0 mg/ml was routinely used in the subsequent binding assays.

The binding of [^{125}I]β-EP was also dependent on the time of incubation (Fig. 3A), although its association process was relatively rapid even at 4°C. In contrast, at 25°C, the [^{125}I]β-EP binding reached maximum at 5 min and gradually decreased with time, due to the degradation of [^{125}I]β-EP during incubation. As shown in Fig. 3B, an excess of unlabeled β-EP rapidly displaced [^{125}I]β-EP from the putative binding sites, while no change was observed after the addition of vehicle only (without unlabeled β-EP). Since there appeared to be two binding compartments from which [^{125}I]β-EP was dissociable with different rates, the data presented in Fig. 3B were analyzed by a nonlinear least-squares regression analysis[28] using the following equation:

$$(\%\text{ of bound } [^{125}\text{I}]\beta\text{-EP}) = a_1 \cdot \exp(-k_1 \cdot t) + a_2 \cdot \exp(-k_2 \cdot t) \qquad (4)$$

where k_1 and k_2 denote first-order dissociation rate constants, and a_1

and a_2 represent relative percent of the two compartments such that $a_1 + a_2 = 100$. Dissociation after 30 min binding leads to values of k_1 and k_2 of 1.48 min^{-1} and 0.0165 min^{-1}, respectively, with a_1 and a_2 being 30.4% and 69.6%, respectively. Obviously, the simulation curve (Fig. 3B) was in a good agreement with the observed data, suggesting the feasibility of a two-compartment model of the ligand dissociation.

Figure 4A shows the specific binding of [^{125}I]β-EP (0.1 nM) to the renal basolateral membranes and the inhibition by various cocentrations of unlabeled β-EP in a series of ten saturation experiments. Since the inhibition curve was biphasic, there appeared to be two binding sites on basolateral membranes, which show high and low affinities to [^{125}I]β-EP. These saturation data were replotted as C_f vs. C_b/P (figure not shown), and the kinetic parameters were calculated by a nonlinear least-squares regression analysis[28] based on a two-binding site model expressed as Eq. 1. Thus, obtained Kd and Bmax values are listed in Table I. Figs. 4B and 4C illustrate the Scatchard plots for β-EP binding at the different concentration ranges of bound β-EP, i.e., 0-7 and 0-0.2 pmol/mg protein, respectively. It can be also inspected from Fig. 4B that the β-EP binding to the renal basolateral membranes consists of two components. The straight lines calculated by Eq. 2 using the obtained kinetic parameters (Table I) were in a good agreement with the observed data points, although the presence of a high-affinity component (depicted in Fig. 4C) is not comprehensively shown owing to its much smaller capacity (0.0331 pmol/mg protein) than the large capacity (7.34 pmol/mg protein) of the low-affinity component. While there is a degradation mechanism of polypeptides called "receptor-mediated degradation"[32,33] by which

peptides can only be degraded after binding with its receptors, there is another type of metabolism of neuropeptides[34] by which the peptides can only be degraded after dissociation from its receptors and then diffusion from the vicinity of the receptors to inactivating peptidases. Taking into consideration that enkephalins are degraded *via* the latter mechanism,[35] it is a likely assumption that [^{125}I]β-EP is also rapidly degraded upon exposure to isolated renal basolateral membranes after dissociation from its receptors, in the absence of peptidase inhibitors.

In terms of Akaike's Information Criteria (AIC),[36] the binding of β-EP to the basolateral membranes was better predicted by assuming two binding sites (AIC = -17.3) rather than assuming only one binding site (AIC = -7.2). Therefore, although the estimated Kd_1 and $Bmax_1$ values were not sufficiently reliable, it is most feasible to conclude the presence of two different classes of specific binding sites on the renal basolateral membranes. The high-affinity, low-capacity binding site may well be a population of opioid receptors, as judged by the small Kd value similar to that (2.5 nM) reported previously for tritiated β-EP binding to brain synaptic membranes at 5°C.[37]

The effects of several opioid ligands on the total binding of [^{125}I]β-EP to the renal basolateral membranes are illustrated in Fig. 5. Of special note is the observsation that naloxone (both 1 μM and 10 μM) and DADLE (10 μM) did not exhibit significant inhibitory effects on the [^{125}I]β-EP binding, while 10 μM of dynorphin(1-13) showed a significant inhibition to the same extent (approximately 50%) with that by 10 μM of β-EP. The inability of naloxone and D-Ala^2-D-Leu^5-enkephalin to inhibit the [^{125}I]β-EP binding leads to suggest that a non-opioid component, which is defined as the specific binding

of opioid peptides insensitive to naloxone, is involved in the [^{125}I]β-EP binding to basolateral membranes. Moreover, taking into considering that the non-opioid bindings of β-EP have been characterized as having low affinities to target cells or proteins such as 34 nM in adrenal medullary membranes,[3] 61 nM in heparin-treated human plasma[7] and 100 nM in cultured human lymphocytes,[9] the observed low-affinity, high-capacity binding site (Kd, 210 nM; Bmax, 7.34 pmol/mg protein) on the renal basolateral membranes could be considered to be non-opioid in nature. Since no opioid-insensitive component of [^{125}I]β-EP binding was seen in the rat brain[3], it is unlikely that the opioid-insensitive component found in the basolateral membranes resulted artificially from the iodination of β-EP. This is also evidenced by the finding that binding characteristics of β-EP monoiodinated at Tyr^{27} are indistinguishable from that of β-EP,[38] while β-EP iodinated at Tyr^{27} as well as at the biologically active N-terminal tyrosine (Tyr^{1}) retains little specific binding activity to the brain synaptic mambranes.[2]

Fig. 5 also indicates that 10 μM of dynorphin(1-13) significantly inhibited the [^{125}I]β-EP binding to basolateral membranes by 50%, suggesting that some region of the β-EP molecule, excluding at least the NH_2-terminal enkephalin sequence, is of particular importance for the [^{125}I]β-EP binding. Considering that the COOH-terminal sequence of the β-EP molecule is essential for the non-opioid component of [^{125}I]β-EP binding to several types of cells, membranes and proteins[3,7-9] a COOH-terminal fragments may well be also important for the non-opioid β-EP binding to renal basolateral membranes. The presence of β-EP in serum and the existence of non-opoioid specific

receptors on the renal basolateral membranes suggest that β-EP may mediate some peripheral physiological functions in the kidney, by mechanisms distinct from those associated with traditional opioid receptors.

In conclusion, we have shown for the first time the exsitence of two different classes of specific binding sites for β-EP on the renal basolateral membranes, and the high- and low-affinity bindings may well be attributed to opioid and non-opioid receptors, respectively. These results are consistent with a possible physiological role of β-EP in the peritubular curculation, which requires further investigation.

Acknowledgements The authors thank Dr. I. Tamai for his technical advice on the preparation of renal basolateral membranes. This study was supported by a Grant-in-Aid for Scientific Research from the Ministry of Education, Science and Culture of Japan, and Project Research Fund from the Graduate School of Natural Science and Technology, Kanazawa University.

REFERENCES

1. C.H. Li: β-Endorphin. *Cell* **31**, 504-505 (1982).
2. H. Sato, Y. Sugiyama, Y. Sawada, T. Iga and M. Hanano: In vivo evidence for the specific binding of human β-endorphin to the lung and liver of the rat. *Biochem. Pharmacol.* **37**, 2273-2278 (1988).
3. K. Kamikubo, H. Murase, M. Murayama, K. Miura, M. Nozaki, and K. Tsurumi: Opioid and non-opioid binding of β-endorphin to bovine adrenal medullary membranes. *Regulatory Peptides* **15**, 155-162 (1986).
4. J.R. Dave, N. Rubinstein, and R.L. Eskay: Evidence that β-endorphin binds to specific receptors in rat peripheral tissues and stimulates the adenylate cyclase-adenosine 3',5'-monophosphate system. *Endocrinology* **117**, 1389-1396 (1985).
5. F.M. Leslie, C. Chavkin, and B.M. Cox: Opioid binding properties of brain and peripheral tissues: evidence for heterogeneity in opioid ligand binding sites. *J. Pharmacol. Exp. Ther.* **214**, 395-402 (1980).
6. J. Garzón, R. Schulz, and A. Herz: Evidence for the -type of opioid receptor in the rat vas deferens. *Mol. Pharmacol.* **28**, 1-9 (1985).
7. A. Hildebrandt, L. Schweigerer, and H. Teschenmacher: Characterization and identification of heparin-induced nonopioid-binding sites for β-endorphin in human plasma. *J. Biol. Chem.* **263**, 2436-2441 (1988).
8. M. Westphal and C.H. Li: β-Endorphin: evidence for the existence of opioid and non-opioid binding components for the tritiated human hormone in NG108-15 cells. *Biochem. Biophys. Res. Com.* **122**, 428-433 (1984).

9. E. Hazum, K.J. Chang and P. Cuatrecasas: Specific nonpiate receptors for β-endorphin. *Science* **205**, 1033-1035 (1979).
10. P. Schwandt, W. Richter, and J. Wilkening: In vitro lipolytic activity of porcine β-endorphin not mediated by an opiate receptor. *FEBS Lett.* **100**, 360-362 (1979).
11. Z. Taylor, D.S. Emmanouel, and A.I. Katz: Insulin binding and degradation by luminal and basolateral tubular membranes from rabbit kidney. *J. Clin. Invest.* **69**, 1136-1146 (1982).
12. E. Sack and Z. Taylor: High affinity binding sites for epidermal growth factor (EGF) in renal membranes. *Biochem. Biophys. Res. Com.* **154**, 312-317 (1988).
13. M. Horster and M. Sone: Peptide-dependent regulation of epithelial nephron functions. *Klin. Wochenschr.* **67**, 852-857 (1989) (References cited therein).
14. M.R. Hammerman and J.R. Gavin III: Binding of IGF and IGF I-stimulated phosphorylation in canine renal basolateral membranes. *Am. J. Physiol.* **251**, E32-E41 (1986).
15. J. Levy, J.R. Gavin III, S. Morimoto, M.R. Hammerman, and L.V. Avioli: Hormonal regulation of $(Ca^{2+}+Mg^{2+})$ATPase activity in canine renal basolateral membranes. *Endocrinology* **119**, 2405-2411 (1986).
16. M.R. Hammerman: Interaction of insulin with the renal proximal tubular cell. *Am. J. Physiol.* **249**, F1-F11 (1985).
17. M.K. Haddox and D.H. Russell: β-Endorphin is a kidney trophic hormone. *Life Sci.* **25**, 615-620 (1979).
18. D.A. Wall and T. Maak: Endocytic uptake, transport, and catabolism

of proteins by epithelial cells. *Am. J. Physiol.* **248**, C12-C20 (1985).

19. H. Sato, Y. Sugiyama, Y. Sawada, T. Iga, and M. Hanano: Physiologically based pharmacokinetics of radioiodinated human β-endorphin in rats. An application of the capillary membrane-limited model. *Drug Metab. Dispos.* **15**, 540-550 (1987).
20. B. Sactor, I.L. Rosenbloom, C.T. Liang, and L. Cheng: Sodium gradient- and sodium plus potassium gradient-dependent L-glutamate uptake in renal basolateral membrane vesicles. *J. Membrane Biol.* **60**, 63-71 (1981).
21. B.F. Scharschmidt, E.B. Keefe, N.M. Blankenship, and R.K. Ockner: Validation of a recording spectrophotometric method for measurement pf membrane-associated Mg^{-} and Na,K-ATPase activity. *J. Lab. Clin. Med.* **93**, 790-799 (1979).
22. K. Walter and C. Schutt, "Methods Enzymic Analysis," vol II, H.U. Bergmeyer ed., Academic Press, New York, 1974, p. 856.
23. M. Orlowski and A. Meister: Gamma-glutamyl-p-nitroanilide: A new convenient substrate for determination and study of L- and D-gamma-glutamyltranspeptidase activities. *Biochim. Biophys. Acta.* **73**, 676-681 (1963).
24. T.L. Rothstein and J.J. Blum: Lysosomal physiology in tetrahymena: I. Effect of glucose, acetate, pyruvate, and carmine on intracellular content and extracellular release of three acid hydrolases. *J. Cell Biol.* **57**, 630-641 (1973).
25. T.E. King: Preparation of succinate dehydrogenase and reconstitution of succinate oxidase. *Methods Enzymol.* **10**, 322-331 (1967).
26. V. Scalera, C. Storelli, C. Storelli-Joss, W. Haase and H. Murer: A simple and fase method for the isolation of basolateral plasma membranes from rat small intestinal epithelial cells. *Biochem. J.* **186**, 177-181 (1980).
27. M. M. Bradford: A rapid sensitive method for the quantification of microgram quantities of protein utilizing the principle of protein-dye binding. *Anal. Biochem.* **72**, 248-254 (1976).
28. K. Yamaoka, Y. Tanigawara, T. Nakagawa and T. Uno: A pharmacokinetic analysis program (MULTI) for microcomputer. *J. Pharmacobio-Dyn.* **4**, 879-885 (1981).
29. R. Quirion, M.S. Finkel, F.A.O. Mendelsohn, and N. Zamir: Localization of opiate binding sites in kidney and adrenal gland of the rat. *Life Sci.* **33** (Sup. I), 299-302 (1983).
30. R. Simantov, S.R. Childers, and S.H. Snyder: [^{3}H]Opiate binding: anomalous properties in kidney and liver membranes. *Mol. Pharmacol.* **14**, 69-76 (1978).
31. a) S. De la Baume, C.C. Yi, J.C. Schwartz, P. Chaillet, H. Marcais-Collado and J. Constentin: Participation of both "enkephalinase" and aminopeptidase activities in the metabolism of endogenous enkephalins. *Neuroscience* **8**, 143-151 (1983); b) S. De la Baume, C. Gros, C.C. Yi, P. Chaillet, H. Marcais-Collado, J. Constentin and J.C. Schwartz: Selective participation of both "enkephalinase" and aminopeptidase activities in the metabolism of endogenous enkephalins. *Life Sci.* **31**, 1753-1756 (1982)
32. O. Sonne: Receptor-mediated endocytosis and degradation of insulin. *Physiol. Rev.* **68**, 1129-1196 (1988) (References cited therein).
33. S. Gammeltoft: Insulin receptors: binding kinetics and structure-

function relationship of insulin. *Physiol. Rev.* **64**, 1321-1387 (1984) (References cited therein).

34. L.B. Hersh: Reaction of opioid peptides with neutral endopeptidase ("enkephalinase"). *J. Neurochem.* **43**, 487-493 (1984).

35. A. Nagy, L. Graf, and A. Lajtha: Met-enkephalin binding to opiate receptors is not functionally coupled to biodegradation. *Life Sci.* **33**, 835-840 (1983).

36. H. Akaike: An information criterion (AIC). *Math. Sci.* **14**, 5-9 (1976).

37. P. Nicolas, R.G. Hammonds, Jr., S. Gomez, and C.H. Li: β-Endorphin: thermodynamics of the binding reaction with rat brain membranes. *Arc. Biochem. Biophys.* **217**, 80-86 (1982).

38. C.I.A. Toogood, K.G. McFarthing, E.C. Hulme, and D.G. Smyth: $[^{125}I]Tyr^{27}$ β-endorphin: a radio-iodinated derivative of β-endorphin for the study of opiate receptors. *Neuropeptides* **5**, 121-124 (1984).

TABLE I.

Kinetic Parameters for the Specific Binding of $[^{125}I]$β-Endorphin to Rat Renal Basolateral Membranes

Parameter	Estimated value[a)]
$Bmax_1$ (pmol/mg protein)	0.0331 ± 0.0237
$Bmax_2$ (pmol/mg protein)	7.34 ± 0.974
Kd_1 (nM)	0.678 ± 0.736
Kd_2 (nM)	210 ± 43

a) Determined by fitting the C_f vs. C_b/P curve using an iterative nonlinear least-squares regression analysis,[28)] and expressed as the mean ± SD of the estimated parameter.

FIGURE LEGENDS

Fig. 1. *Time Courses of TCA-insolubility (%) of [^{125}I]β-EP during Incubation with Rat Renal Basolateral Membranes.*

[^{125}I]β-EP (0.1 nM) incubated with basolateral membranes (1 mg/ml) for designated time intervals was mixed with 15% TCA, filtered through GF/C filters, and the TCA-insoluble radioactivity on the filter was counted. Each point and vertical bar represent the mean ± SEM (n = 4). ●, at 4°C without peptidase inhibitors; Δ, at 4°C with bestatin 0.1 mM, bacitracin 50 μM and NEM 1 mM; ▲, at 25°C with EDTA 10 mM; ○, at 4°C with EDTA 10 mM.

Fig. 2. *Total and Nonspecific Bindings of [^{125}I]β-EP as a Function of Rat Renal Basolateral Membrane Concentration.*

Protein concentrations between 0.18 and 1.5 mg/ml were incubated with [^{125}I]β-EP (0.1 nM) for 90 min at 4°C in the presence of 10 mM EDTA. Nonspecific binding was determined in the presence of 10 μM unlabeled β-EP. Each point and vertical bar represent the mean ± SEM (n = 3-4). —●—, total binding; --○--, nonspecific binding.

Fig. 3. *Time Courses of Association (A) and Dissociation (B) of [^{125}I]β-EP to Rat Renal Basolateral Membranes.*

In panel B, dissociation of [^{125}I]β-EP (0.1 nM), which was bound to basolateral membranes (1 mg/ml) for 30 min in the presence of 10 mM EDTA, was examined after dilution with (○) and without (●) unlabeled β-EP (10 μM), and the dissociation curve for the displacement of [^{125}I]β-EP by unlabeled β-EP was drawn by a nonlinear least-squares regression analysis[28] according to Eq. 3.

Fig. 4. *Inhibition of Specific Binding of [^{125}I]β-EP to Rat Renal Basolateral Membranes by Various Concentrations of Unlabeled β-EP (A) and Scatchard Plots for [^{125}I]β-EP Binding (B, C).*

[^{125}I]β-EP (0.1 nM) was incubated with basolateral membranes (1 mg/ml) at 4°C for 90 min in the presence of 10 mM EDTA. In panel A, the inhibition curve was drawn by eye fitting. In panels B and C, the ratio of bound [^{125}I]β-EP (pmol/mg protein) to free [^{125}I]β-EP (nM) is plotted against bound [^{125}I]β-EP in both wide (0-7 pmol/mg protein) and narrow (0-0.25 pmol/mg protein) concentration ranges, respectively. The solid lines in panels B and C were drawn by Eq. 3 using the kinetic parameters for the low-affinity binding site, and the dotted line in panel C was plotted for the high-affinity binding site. Each point and bar represent the mean ± SEM (n = 3-5).

Fig. 5. *Effects of Several Opioid Ligands on the [^{125}I]β-EP Binding to Rat Renal Basolateral Membranes.*

[^{125}I]β-EP (0.1 nM) was incubated with basolateral membranes (1 mg/ml) at 4°C for 90 min in the absence and presence of an unlabeled opioid ligand, and the total [^{125}I]β-EP binding was determined. Each column and bar represent the mean ± SEM (n = 5). The significance of differences between the binding experiments in the absence and presence of an unlabeled opioid ligand was assessed by means of Student's *t*-test: * $P < 0.01$.

Fig. 1

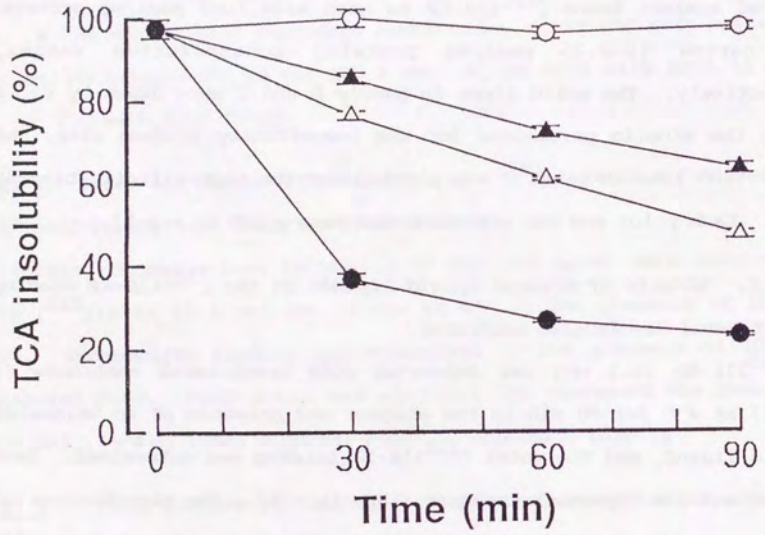
TCA insolubility (%)
100
80
60
40
20
0
0
30
60
90
Time (min)

Fig. 2

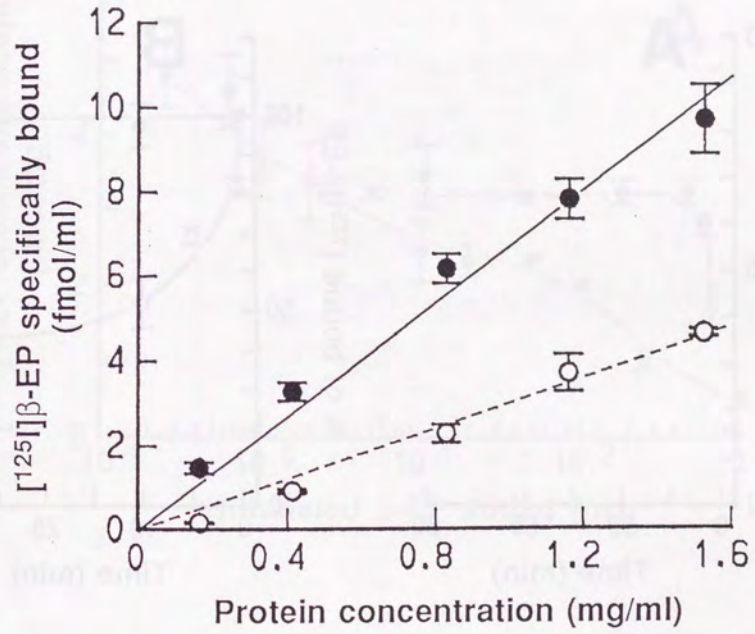
[125I]β-EP specifically bound
(fmol/ml)
12
10
8
6
4
2
0
0
0.4
0.8
1.2
1.6
Protein concentration (mg/ml)

Fig. 3

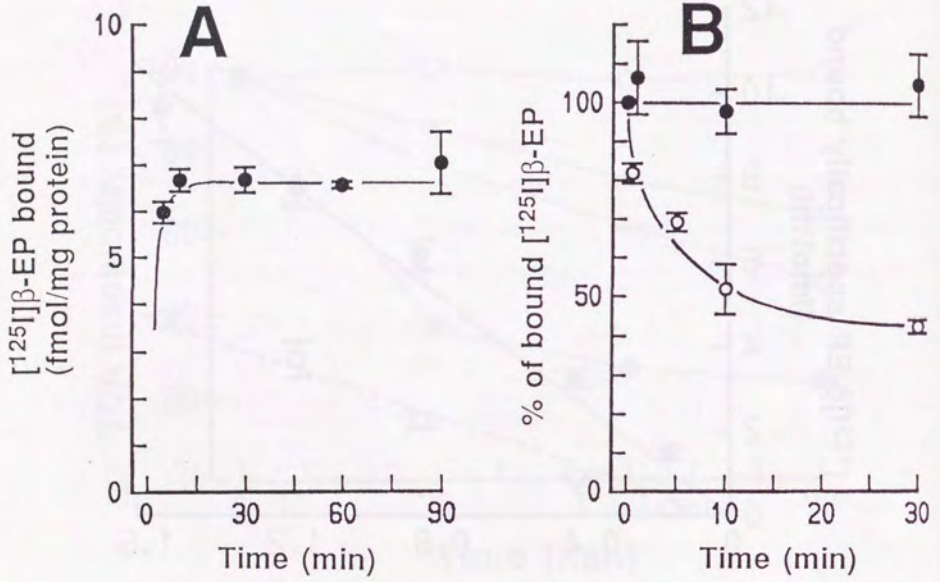
A
B
[125I]β-EP bound (fmol/mg protein)
% of bound [125I]β-EP
Time (min)
Time (min)
0
5
10
30
60
90
50
100
20

Fig. 4

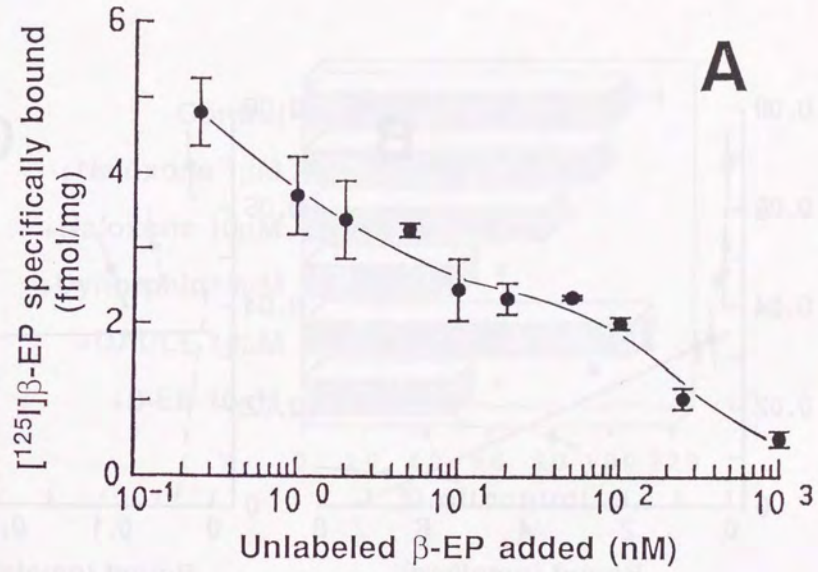
A
[125I]β-EP specifically bound (fmol/mg)
Unlabeled β-EP added (nM)
0
2
4
6
10−1
10 0
10 1
10 2
10 3

Fig. 4

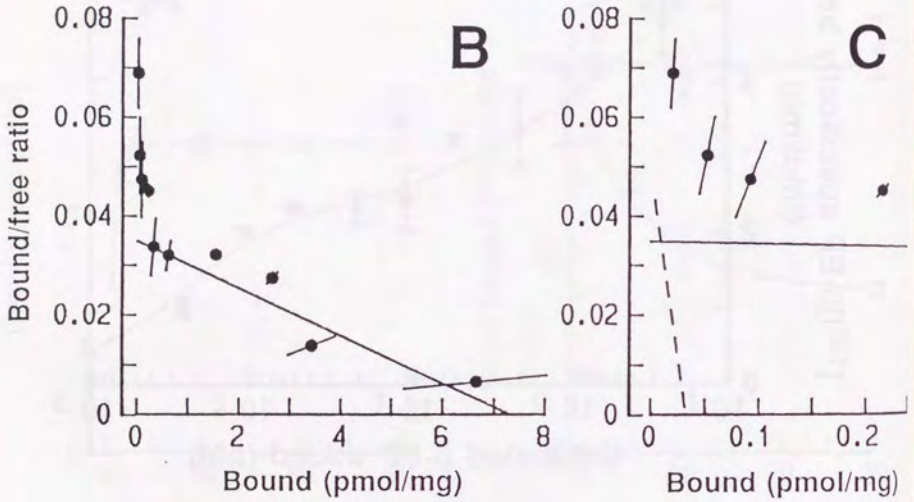
B
C
Bound/free ratio
0.08
0.06
0.04
0.02
0
0 2 4 6 8
Bound (pmol/mg)
0 0.1 0.2
Bound (pmol/mg)

Fig. 5

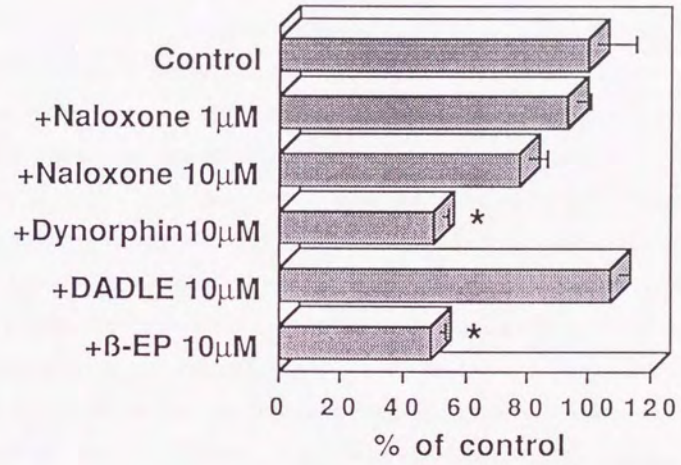
Control
+Naloxone 1μM
+Naloxone 10μM
+Dynorphin10μM
+DADLE 10μM
+ß-EP 10μM
*
*
0 20 40 60 80 100 120
% of control